Palaeogeography, Palaeoclimatology, Palaeoecology 506 (2018) 48–69

Contents lists available at ScienceDirect

Palaeogeography, Palaeoclimatology, Palaeoecology

journal homepage: www.elsevier.com/locate/palaeo

# Magneto-biostratigraphy and paleoenvironments of the Miocene freshwater sediments of the Sarajevo-Zenica Basin

Sant K.[a,*], Andrić N.[a,b], Mandic O.[c], Demir V.[e,a], Pavelić D.[d], Rundić Lj.[b], Hrvatović H.[e], Matenco L.[a], Krijgsman W.[a]

[a] Utrecht University, Paleomagnetic Laboratory 'Fort Hoofddijk', Budapestlaan 17, 3584 CD Utrecht, the Netherlands
[b] University of Belgrade, Faculty of Mining and Geology, Serbia
[c] Natural History Museum Vienna, Geological-Paleontological Department, Austria
[d] University of Zagreb, Faculty of Mining, Geology & Petroleum Engineering, Croatia
[e] Geological Survey of the Federation of Bosnia and Herzegovina, Bosnia and Herzegovina

ARTICLE INFO

*Keywords:*
Lacustrine basin
Dinarides
Chronology
Paleoclimate
Syn-sedimentary extension

ABSTRACT

The Sarajevo-Zenica Basin of Bosnia-Herzegovina was part of the Dinaride Lake System, a large network of Miocene long-lived freshwater basins in southeastern Europe. The basin contains a thick sedimentary succession of carbonates, coals and mixed siliciclastic deposits that reflects the paleoclimatic and tectonic evolution of the region. In this study, we present novel integrated (magneto-bio)stratigraphic and sedimentological data and reconstruct the paleoenvironmental evolution of the Sarajevo-Zenica Basin during its two main evolutionary phases (thrusting and extension). The basal "Oligo-Miocene" freshwater paleoenvironments are characterized by alternating palustrine, shallow lacustrine and distal fluvial phases. The base level fluctuations are largely controlled by syn-sedimentary pulses of tectonic loading during the final phase of thrusting in the Internal Dinarides. The majority of this succession is considered early Miocene in age, which contrasts with previous Oligocene age estimates. The subsequent extensional phase initiated not later than ~18.4 Ma. This coarsening upward sequence of lacustrine carbonates, silts, sands and conglomerates is correlated between 17.2 and 15 Ma (C5Cr-C5Br) by means of integrated bio-magnetostratigraphy. During this upper extensional phase, subsidence and sediment influx was generally controlled by activity along the basin bounding normal fault, overruling smaller scale climatic influences. We conclude that the existence of the long-lived Sarajevo lake is coeval with other Dinaric and southern Pannonian lakes, and overlaps in time with the Miocene Climatic Optimum. Sedimentation in the Sarajevo-Zenica basin terminated at ~15–14 Ma which concurs with both the end of the climatic optimum as well as the cessation of extension in the Dinarides. These results will help to better quantify the paleoclimatic changes in the Dinaride Lake System as well as the regional tectono-sedimentary events, such as potential migrations of deformation across the Dinarides.

## 1. Introduction

During the Miocene, a system of long-lived freshwater basins developed in the Dinarides mountains of Central Europe (the Dinaride Lake System, DLS), which was located between the Central Paratethys and proto-Mediterranean realms (Fig. 1) (Harzhauser and Mandic, 2008; Krstić et al., 2012; Mandic et al., 2012). The formation and evolution of this intra-montane lake system partly overlaps and was influenced by two major events that affected the Dinarides, namely a period of regional Oligocene-Miocene extension (Erak et al., 2017; Toljić et al., 2013; Ustaszewski et al., 2010) and a temporary change in global climate that created a generally wet and hot period called the Miocene Climatic Optimum (MCO; ~17–15 Ma) (Holbourn et al., 2015; Zachos et al., 2001). The latter is commonly considered to be an important factor for sustaining the paleoenvironments of the DLS (de Leeuw et al., 2010, 2011b; Mandic et al., 2011), but recent structural and sedimentological observations have shown that tectonics might have played a more important role than previously assumed (Andrić et al., 2017).

The isolated paleogeographic position and warm climate enabled a spectacular speciation and adaptive radiation of its endemic freshwater fossils. Over a 100 endemic mollusk species have been described so far (Harzhauser and Mandic, 2008; Neubauer et al., 2015b). The DLS was also home to predecessors of present-day Mediterranean flora (Jiménez-

* Corresponding author.
*E-mail address:* k.sant@uu.nl (K. Sant).

https://doi.org/10.1016/j.palaeo.2018.06.009
Received 16 February 2018; Received in revised form 4 June 2018; Accepted 5 June 2018
Available online 08 June 2018
0031-0182/ 

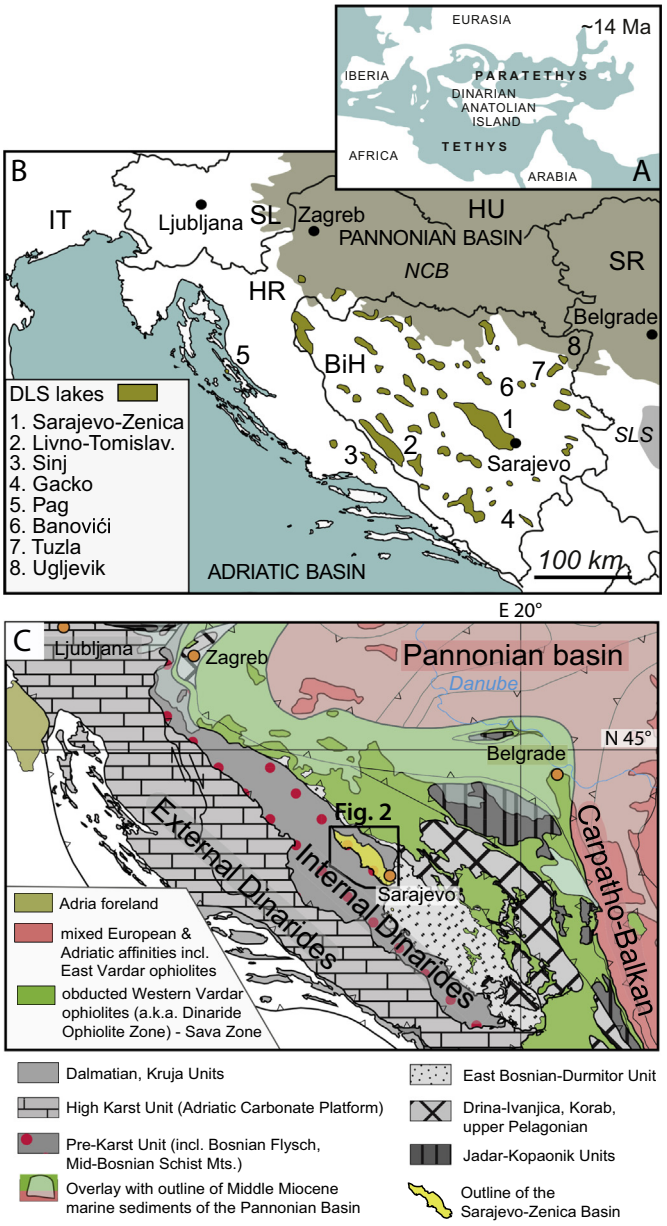


**Fig. 1.** Position of the Sarajevo-Zenica Basin (A) Paleogeography of the Dinaride block ~14 Ma. (B) Present-day extent of the Dinaride Lake System (DLS) and Pannonian Basin deposits drawn on the present-day geographic map of south-eastern Europe (modified after Mandic et al., 2011). NCB = North Croatian Basin, SLS = Serbian Lake System. (C) Tectonic map of south-eastern Europe (Ustaszewski et al., 2008) depicting the most prominent tectonic terranes and the outline of the Sarajevo-Zenica Basin sediments.
Adapted after Andrić et al. (2017).

Moreno et al., 2009). The lake basins are generally excellent recorders of such fauna, flora, and variability in climate (such as precipitation or temperature), while often good preservation of tectonic structures allows a good reconstruction of the kinematic evolution (e.g., Albrecht and Wilke, 2008; Andrić et al., 2017; Cohen, 2003a; Jiménez-Moreno et al., 2008; Mandic et al., 2011; Neubauer et al., 2015b). In such environments, the interplay between climate, tectonics and fauna speciation can be derived, but their timing must be quantified by high resolution chronostratigraphy.

Therefore, many DLS successions were recently dated by use of integrated methods including magnetostratigraphy, radioisotopic dating and cyclostratigraphy (de Leeuw et al., 2010, 2011b; Jiménez-Moreno et al., 2009; Mandic et al., 2012). This allowed a quantitative comparison between different basins and enhanced understanding of the paleoenvironmental and paleobiogeographic evolution of the Dinarides and adjacent regions (Mandic et al., 2012; Neubauer et al., 2015a). Most of these stratigraphic studies focused on the Miocene DLS basins situated on the limestone-rich High Karst terranes of the External Dinarides (de Leeuw, 2011; Mandic et al., 2009, 2011) (Fig. 1). Miocene sedimentation in these basins was dominated by intra-basinal deposition of carbonates with relatively low terrigenous input. In contrast, deposition in basins located in the Internal Dinarides was often interrupted by land-derived coarser siliciclastic sediments sourced from the surrounding ophiolites and metamorphic units, which are often less suitable for high resolution chronostratigraphy.

The largest and thickest among the numerous DLS basins presently preserved is the Sarajevo-Zenica Basin, located in the external part of the Internal Dinarides (Fig. 1, Aubouin et al., 1970). The sediments are distributed over an elongated 20 by 70 km area and are > 3 km thick (Dragičević et al., 2010; Milojević, 1964). A large part of the basin infill is dominated by siliciclastic material that accumulated during three evolutionary phases (sensu Andrić et al., 2017) (Fig. 2). The first "Oligo-Miocene" (i.o.w. latest Oligocene-early Miocene) phase is characterized by palustrine-fluvial deposits that were most probably deposited in a shallow foredeep basin formed in the footwall of the main East Bosnian – Durmitor unit during its latest stages of thrusting over the Bosnian Flysch turbidites (Fig. 1C) (Andrić et al., 2017). The overlying early-middle Miocene lacustrine-alluvial succession (a.o. the Lašva conglomerates and sandstones in Fig. 2A) accumulated during the large scale extensional event affecting the Dinarides. The third evolutionary phase recorded the deposition of late Miocene-Pliocene palustrine-fluvial deposits that recorded the gradual thrusting and inversion of the Sarajevo-Zenica Basin (Andrić et al., 2017; Milojević, 1964; Muftić, 1965; Pantić et al., 1966).

In this study, we place the paleoenvironmental evolution of the central Sarajevo-Zenica Basin in the context of the regional tectonic and climatic changes that affected the basin during the earlier thrusting and later extensional evolution by means of a detailed stratigraphic study of the Oligocene-Miocene lithological succession. We developed an integrated chronostratigraphic framework based on magnetostratigraphy, biostratigraphy and lithostratigraphy, focused on areas as distal as possible from the basin margin to avoid interruption of land-derived coarse-grained sediments (Fig. 2). The newly obtained record will substantially improve the understanding of the paleoenvironmental evolution of the Sarajevo-Zenica Basin and its relationship to other basins in the larger framework of the Dinaride Lake System. These data will allow a quantitative comparison between changes in basin stratigraphy and regional tectono-climatic events, such as potential migrations of deformation across the Dinarides.

## 2. Geological background

### 2.1. Tectonic history of the Dinarides and its surroundings

During the Oligo-Miocene, the Dinaride-Anatolian block formed a paleogeographic barrier between the Central Paratethys and Mediterranean realms, and was an important land bridge for mammal migration from Asia to Europe (Fig. 1A) (e.g., de Bruijn et al., 2017; Koufos et al., 2003). DLS palynological records show that the relief of the Dinaride mountains exceeded 1000 m in early-middle Miocene times (Jiménez-Moreno et al., 2008, 2009). This high relief separating the large-scale realms has allowed the formation of a number of intramontane lakes, often overlapping lower altitude tectonic contacts. The Sarajevo-Zenica Basin is one such large lake, whose sediments cover the highly deformed contact zone of the Bosnian Flysch turbidites, which formed in the footwall of the large thrusting carrying the composite continental units overlain by obducted ophiolites of the Internal Dinarides (the thrust between the East Bosnian – Durmitor and pre-Karst units in Figs. 1C, 2A).

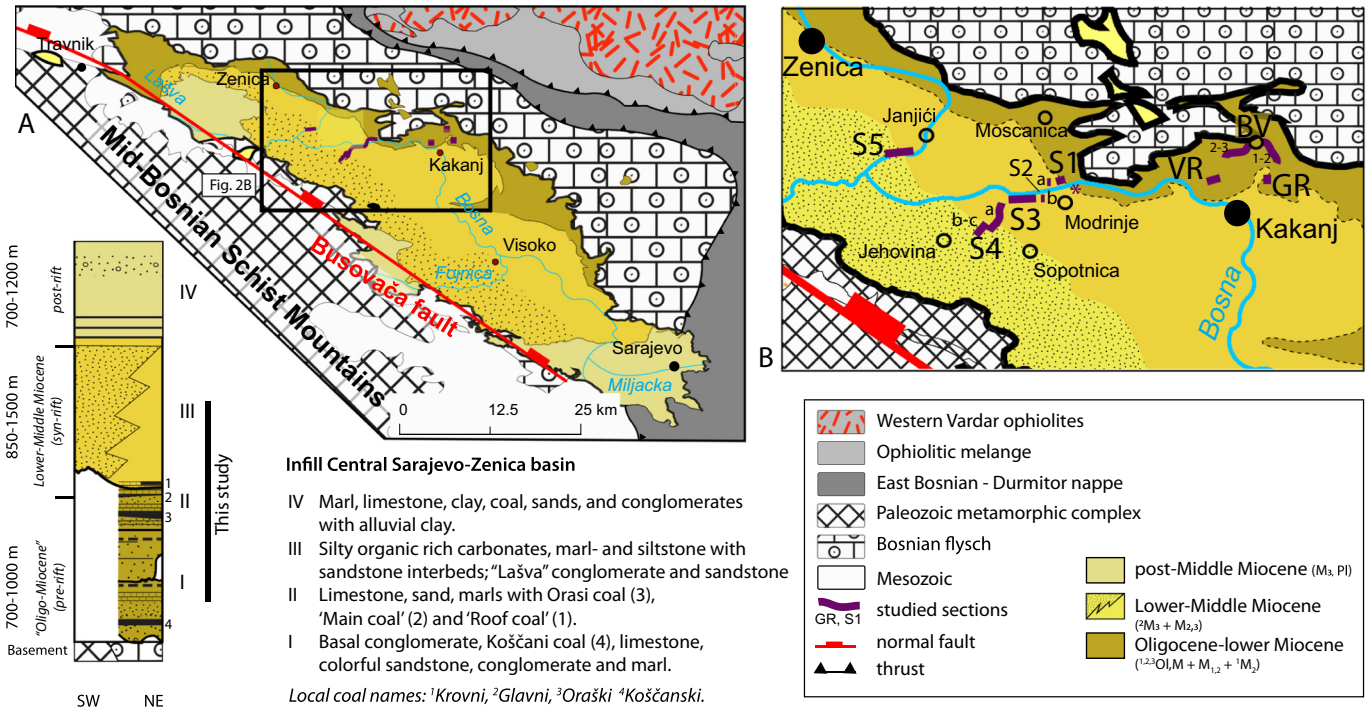


**Fig. 2.** Geology of the Sarajevo-Zenica Basin (A) Geological map of the Sarajevo-Zenica Basin plus surrounding tectonic terranes, study areas and generalized basin infill for the central part (Jovanović et al., 1971; Milojević, 1964; Olujić et al., 1978; Sofilj and Živanović, 1971; Živanović et al., 1967). See the main text for a detailed account of the units and lithologies. (B) Magnification of the central part of the basin with locations of the studied sections (S = section; GR = Greben, VR = Vrtlište, BV = Bijele Vode, * = oncoid-sands depicted in Fig. 5A). See legend for details, including the original terms used on the geological map. Modified after (Andrić et al., 2017) and geological maps by (Jovanović et al., 1971; Olujić et al., 1978; Sofilj and Živanović, 1971; Živanović et al., 1967).

The Dinarides formed in response to the Middle Triassic continental rifting followed by the opening of a northern branch of the Neotethys Ocean that separated Adriatic-derived (i.e., Dinarides) and Europe-derived continental units. Its subsequent orogenic closure started in the Middle Jurassic (Schmid et al., 2008). One marked moment of this ocean closure was the Late Jurassic – earliest Cretaceous obduction of ophiolites and genetically associated ophiolitic mélanges over the Adriatic continental margin (the Western Vardar Ophiolitic units of Schmid et al., 2008, a.k.a. Dinaride Ophiolite Zone, see also Hrvatović, 2006; Pamić et al., 2002; Ustaszewski et al., 2008). This thrusting was associated with the onset of deposition in the Bosnian Flysch zone, a long sedimentary belt that can be mapped from the Southern Alps to the Albanides, composed of turbidites and other mass flow deposits interbedded with more pelagic sediments located in the frontal part of the obducted continental units (Fig. 1C). In this Bosnian Flysch Zone, the Late Jurassic – earliest Cretaceous deposition is grouped under the generic name of the Vranduk Flysch Fm., while later thrusting reactivations of this tectonic contact have resulted in the locally unconformable Cretaceous deposition of the Ugar Flysch Fm., or its lateral Durmitor Flysch equivalent of Montenegro (Dimitrijević, 1997; Hrvatović and Pamić, 2005; Mikes et al., 2008; Rampnoux, 1970).

Large scale shortening affected the Dinarides during multiple Cretaceous-Oligocene events that peaked during the latest Cretaceous formation of the Sava Zone, which is the suture zone between the Dinarides and Europe-derived units (Fig. 1C) (Andrić et al., 2017; Schmid et al., 2008; Ustaszewski et al., 2010). This shortening was characterized by the formation of the SW-vergent Dinarides nappe stack, where its various thrusted units are generally grouped in Internal (from NE to SW Jadar - Kopaonik, East Bosnian – Durmitor, Drina – Ivanjica and pre-Karst) and External (from NE to SW High Karst, Budva and Dalmatian) Dinarides units (Aubouin et al., 1970; Hrvatović and Pamić, 2005; Schmid et al., 2008).

The Dinarides and its margins were affected by a widely observed period of late Oligocene - Miocene extension that generally reactivated inherited rheologically weak zones such as nappe contacts or sutures (Stojadinović et al., 2013; Tari and Pamić, 1998; Toljić et al., 2013; van Unen et al., 2017). Extensional deformation started in the Oligocene (~29 Ma) near the Sava Zone (Erak et al., 2017), and gradually migrated in space and time towards more external parts of the orogen, where it peaked during middle Miocene times (Andrić et al., 2017). Dinarides extension was partly coeval with the one of the much larger Pannonian Basin situated to the north, which started the earliest at ~20 Ma and peaked at ~15–14 Ma (Fodor et al., 1999; Horváth et al., 2015; Matenco and Radivojević, 2012; Stojadinović et al., 2013). In the Dinarides and their northern margin with the Pannonian Basin, the extension reactivated inherited nappe and suture zone contacts and created asymmetric basins controlled by detachments or low-angle normal faults associated with crustal scale exhumation of their footwalls (Stojadinović et al., 2013; Ustaszewski et al., 2010). A few lakes in the northern Dinarides (e.g., Banovići, Ugljevik; Fig. 1B) formed already during late Oligocene times (de Leeuw et al., 2011a; Wessels et al., 2008), but the majority formed after 18 Ma (e.g., de Leeuw et al., 2012; Mandic et al., 2011). The Dinarides were affected by the northward movement of Adria and their indentation starting with the latest Miocene (~8 Ma, e.g., Ustaszewski et al., 2014), which inverted and exhumed the last remainders of the Dinarides lakes.

### 2.2. Tectono-sedimentary history of the Sarajevo-Zenica Basin

All tectonic events related to the evolution of the Sarajevo-Zenica Basin were influenced by the rheological weakness of the Bosnian Flysch sediments, thrusted beneath the East Bosnian – Durmitor unit, which resulted in the formation of either thrusts or normal faults that follow this generally NE to N-ward dipping contact (Figs. 1C, 2A, Andrić et al., 2017). The Oligocene foredeep thrusting was followed by the early-middle Miocene formation of an asymmetric basin (=syn-rift phase) along a NE-ward dipping listric normal fault system (the Busovača Fault system, Fig. 2B) that was associated with 7–8 km of

exhumation of the Mid-Bosnian Schist Mountains to the SW of the Sarajevo-Zenica Basin (Casale, 2012). In this process, the Paleozoic metamorphic rocks of the Mid-Bosnian Schist core complex emerged together with Triassic dolomites and Devonian dolomitic limestones (Hrvatović, 2006; Jovanović et al., 1971). This extension has created a succession of syn-kinematic depositional wedges formed in the hanging-wall of each normal fault with coarse continental alluvial to shallow deltaic proximal sedimentation and turbiditic to more pelagic sedimentation in more distal areas of the basin (Fig. 2B). Similarly with other areas of the Dinarides (Tomljenović and Csontos, 2001; Ustaszewski et al., 2014), the Sarajevo-Zenica Basin was inverted and gradually exhumed starting with the latest Miocene onset of the Adriatic indentation, which folded the basin sediments and reactivated the previous normal faults as low-angle thrusts (Andrić et al., 2017; Muftić and Luburić, 1963).

The existing chronostratigraphy of the sedimentary infill (Fig. 2A) is mainly based on regional plant, mammal and mollusk stratigraphy (Kochansky-Devidé and Slišković, 1972, 1978; Pantić et al., 1964, 1966; Pantić, 1956, 1961, 1962; Pantić and Bešlagić, 1964; Weyland et al., 1958). The basal coal ("Koščani coal") was correlated with late Oligocene localities such as Socka in Slovenia (Bechtel et al., 2004) or Bogovina in Serbia (Utescher et al., 2007). The "Main coal seam" (Fig. 2A) was attributed to the early/middle Miocene, based on palynological data and fossil mammal remains encountered in the Vrtlište coal mine, which belong to the *Deinotherium cuvieri bavaricum* lineage (MN4-MN6 zone, i.e. ~17.6–12.7 Ma by Pickford and Pourabrishami, 2013; ~18.1–13.2 Ma by Böhme et al., 2012) (Milojković, 1929) (Fig. 2A). The subsequent lacustrine phase was correlated with the middle Miocene based on thermophile pollen and macroflora, whereas mollusks indicated an early to middle Miocene age (Kochansky-Devidé and Slišković, 1972, 1978; Pantić et al., 1966). The post-rift successions were tied to the late Miocene to lower Pliocene (Pantić et al., 1966).

The basin infill of the Sarajevo-Zenica Basin was studied by Milojević (1964) and Muftić (1965). Milojević (1964) defined several transgressive-regressive successions (TRS) (Table 2). The first succession comprises: (a) conglomerates and clays (100 m), (b) Koščani coal seam, limestone and marl (170 m), (c) red conglomerates, sands and clay (600 m), and (d) bituminous tuffaceous limestone (200 m). The second succession comprises: (a) Main Coal Unit composed of a lower sub-unit ($a_1$) with coal, sand, silt and clay (300 m), a middle sub-unit ($a_2$) Orasi and Main coal seams (120 m) and an upper sub-unit ($a_3$) with a thin coal seam intercalated between *Carpolithes* and *Glyptostrobus* limestone (70 m). On top follows (b) a Transitional Unit dominated by marl and sandstone (600 m) and (c) Lašva Formation bearing sands and conglomerates (1000 m). Muftić (1965) defined 8 units that are very similar to those of Milojević (1964). Most importantly, a *Delminiella (= "Velutinopsis")* zone (Unit 7, ~200 m) was recognized corresponding to the lower marls of the Transitional Unit (sensu Milojević). The author demonstrated that the Lašva Fm. and Transitional Unit are largely synchronous, as recently confirmed by Andrić et al. (2017) (Fig. 2A).

The "Oligo-Miocene" and lower-middle Miocene successions of this study correspond approximately to the TSR1-TSR2$a_2$ and TSR2$a_3$-c sequences by Milojević (1964), and to Units 1–4 and 5–8, respectively, by Muftić (1965) (Table 2).

## 3. Stratigraphic methods and sampling

The lowermost "Oligo-Miocene" freshwater succession was studied by field logging of sections and short isolated outcrops, supplemented by literature and drill core data derived from the open pit mining area Kakanj (Figs. 2–4). Most information was derived from the Bijele Vode section (BV1–2) and (the accessible parts of the) Vrtlište mine (VR; Fig. 3). The younger extensional lake succession was studied in the Greben mine (GR) and in the Modrinje-Janjići composite section. The latter was constructed from five partial sections (S1–5) of railway and road outcrops in the SSW part of the Sarajevo-Zenica Basin (Figs. 2, 3, 5).

The majority of studied areas consist of relatively fine-grained sediments with various macro- and microstructures that help to reconstruct the paleoenvironmental evolution of the basin. For this purpose, hand specimens were collected for microanalysis, and thin slides were produced in the GeoLab Facility of the Faculty of Geosciences of Utrecht University.

Biostratigraphic and paleoenvironmental investigations focused mainly on ostracods and mollusks. Six samples were collected throughout the basin for ostracod analyses and six samples for mollusk analysis. All samples were processed following standard preparation techniques. Ostracods were generally poorly preserved, and most determinations were based on fragments, recrystallized carapaces and imprints. Determinations were mainly done on the generic level, because taxonomic criteria, such as marginal pore canals, were often absent. The ostracods were photographed and stored in the Regional Geology Department of the Faculty of Mining and Geology, Belgrade University (collection code SA-OSTR2014). See Table 1 for an overview of the biostratigraphic data and sample localities. The mollusk samples are stored in the stratigraphic collection (number: NHMW 2018/0153) of the Natural History Museum in Vienna.

Standard oriented paleomagnetic cores were drilled in exposed parts of the Modrinje-Janjići profile at a resolution of 1 m, except for S5 where cores were drilled every 5 m. This resulted in a total amount of 548 sampled magnetostratigraphic levels (one or two cores per level). Additionally, 78 samples were taken from intervals in the coaly and carbonatic sections in Vrtlište and Greben mines. Paleomagnetic sampling took place during September–October 2014 and October 2015.

Additionally, several tuffs were sampled (> 1 kg) for $^{40}Ar/^{39}Ar$ radioisotopic dating. Unfortunately, most samples showed signs of reworking, such as rounded grains and many sheet silicates, and were not processed. One feldspar rich sample from level 403 m of S3 was irradiated and measured, but yielded an Eocene age, reflecting the age of transported minerals instead of the eruption age.

## 4. Lithostratigraphy, biostratigraphy and environments

### 4.1. The "Oligo-Miocene" sediments

Oligo-Miocene sediments are exposed along the northern and northwestern boundary of the Sarajevo-Zenica Basin (Fig. 2). The basal part of the oldest freshwater sequence starts with brick-red conglomerates and breccias, and is topped by the "Koščani" coal (= Koščanski ugljeni sloj; Glišić et al., 1976; Milojević, 1964). The basal succession is only exposed north of Gornja Breza and Ponihovo (between Kakanj and Zenica). The overlying siliciclastics and limestones are found in the localities Moščanica, Kraljeva Sutjeska, Podvinjci and Bijele Vode (see below), while the uppermost interval with coal packages is exposed in several coal mines, notably Zenica, Kakanj, Breza and Nova Bila near Travnik (see below).

#### 4.1.1. Bijele Vode area

The sediments in the Bijele Vode composite section overlie the Koščani coal unit, but the contact is not exposed (Fig. 4A). The lower part of the sequence (~70 m thick) comprises (blue) gray marls with irregularly bedded pack-, wacke-, and mudstones. The basal wacke- and packstones (BV1) contain many plant stems and fossil plant roots coated with organic matter, and stromatolites (Fig. 7A,C,D). Macro- and microscopic observations show the omnipresence of mottling, micro cracks, hematite spots and nodular limestone levels. Microanalysis shows that part of the rocks are microbialites with clotted structures of bacteria, honey comb structures, algae oncoids and tabular microstructures (*Porostromate*) (Fig. 7E,F). The rest of the section (> 9 m) is dominated by blue and brown gray marl with well-preserved organic matter on the bedding. They irregularly alternate with 1–50 cm thick wacke-to-packstones (Fig. 4). Most limestone levels pinch out (max.

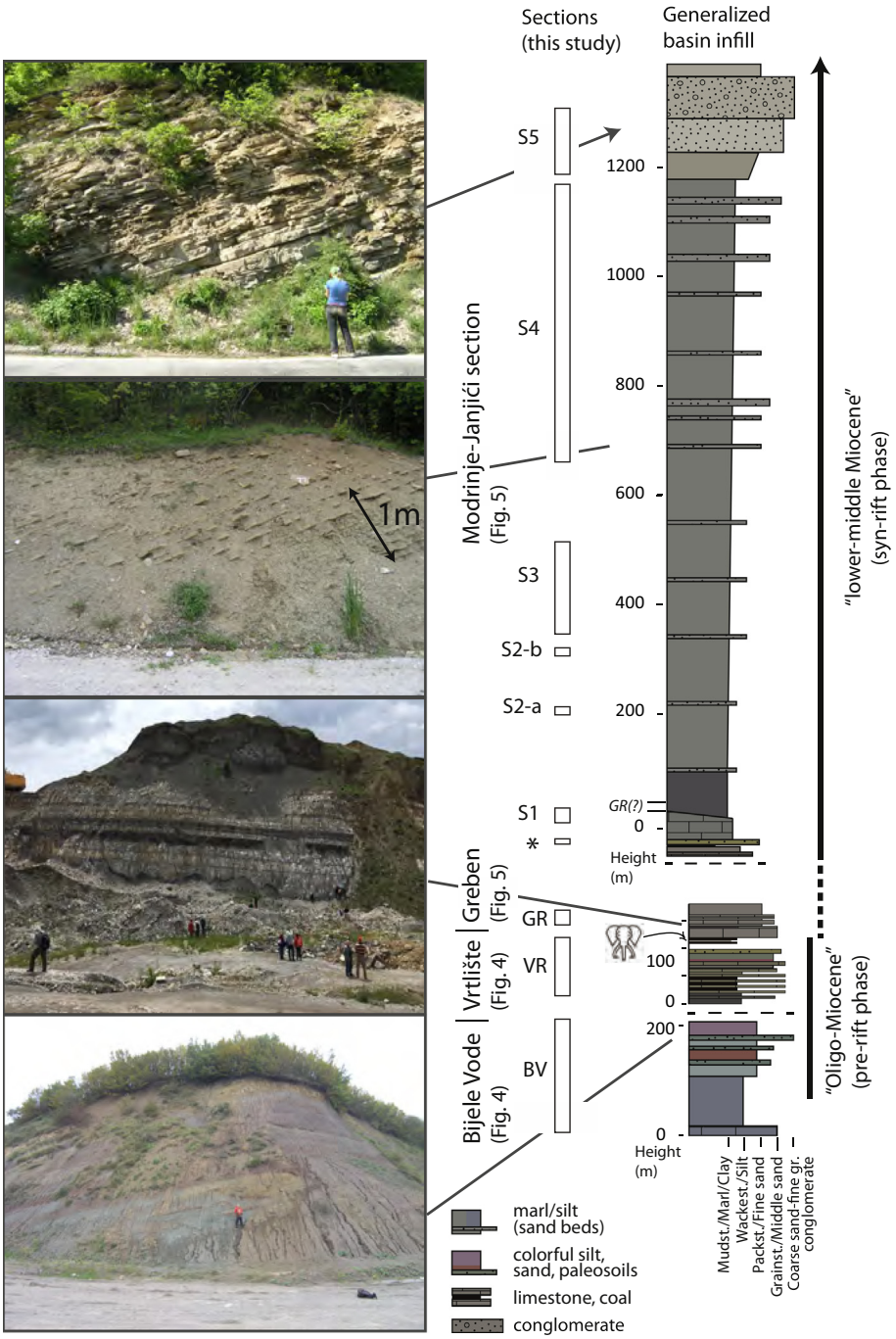


**Fig. 3.** Studied successions. Generalized lithological column and characteristic photographs of the studied succession in the central Sarajevo-Zenica Basin. The studied sections are indicated by vertical bars with abbreviations (S1 = section 1, S2 = section 2 etc.). The most likely correlation of GR to the Modrinje section is indicated. See the main text for an explanation of the basin phases and successions. Colors are similar to the colors in the field; see the legend in Fig. 4 for an explanation of the lithological patterns. The elephant head marks the finding of *Deinotherium*.

~5–20 m wide).

Common large *Pisidium* sp. shells and ostracod remains were encountered together with decomposed mud clasts in the basal part of BV1 (7 m). The ostracod assemblage (sample R1) includes *Amplocypris* sp., *Fabaeformiscandona* sp., *Candonopsis* sp., *Limnocythere* sp., *Paralimnocythere* sp. and various *Candonas* (Fig. 6K,L; Table 1). The marlstones in the top of BV1 (61 m; sample R2) yield large specimens of *Heterocypris* (> 1.7 mm) and frequent smaller *Cypridopsis*.

Stromatolites (by cyanobacteria) are most commonly generated in very low energy environments in the photic zone (e.g., Riding, 1991; Stow, 2005). Oncoids reflect coastal conditions of a very shallow lake influenced by river flow and wind (Peryt, 1983). Together with the omnipresence of emersion features, such as mottling, micro cracks and algae oncoids, this indicates palustrine conditions for the lowermost BV1 (Alonso-Zarza and Wright, 2010; Freytet and Verrecchia, 2002). The overlying marl-dominated interval represents slightly deeper littoral lake conditions where organic matter is often well-preserved pointing to lake stratification (e.g., Cohen, 2003d; Whelan and Farrington, 1992). *Pisidium* and the ostracod assemblage confirm the shallow lacustrine to palustrine setting (Meisch, 2000; Witt, 2002, 2011).

The upper part of the Bijele Vode section (BV2) (~100 m thick) is

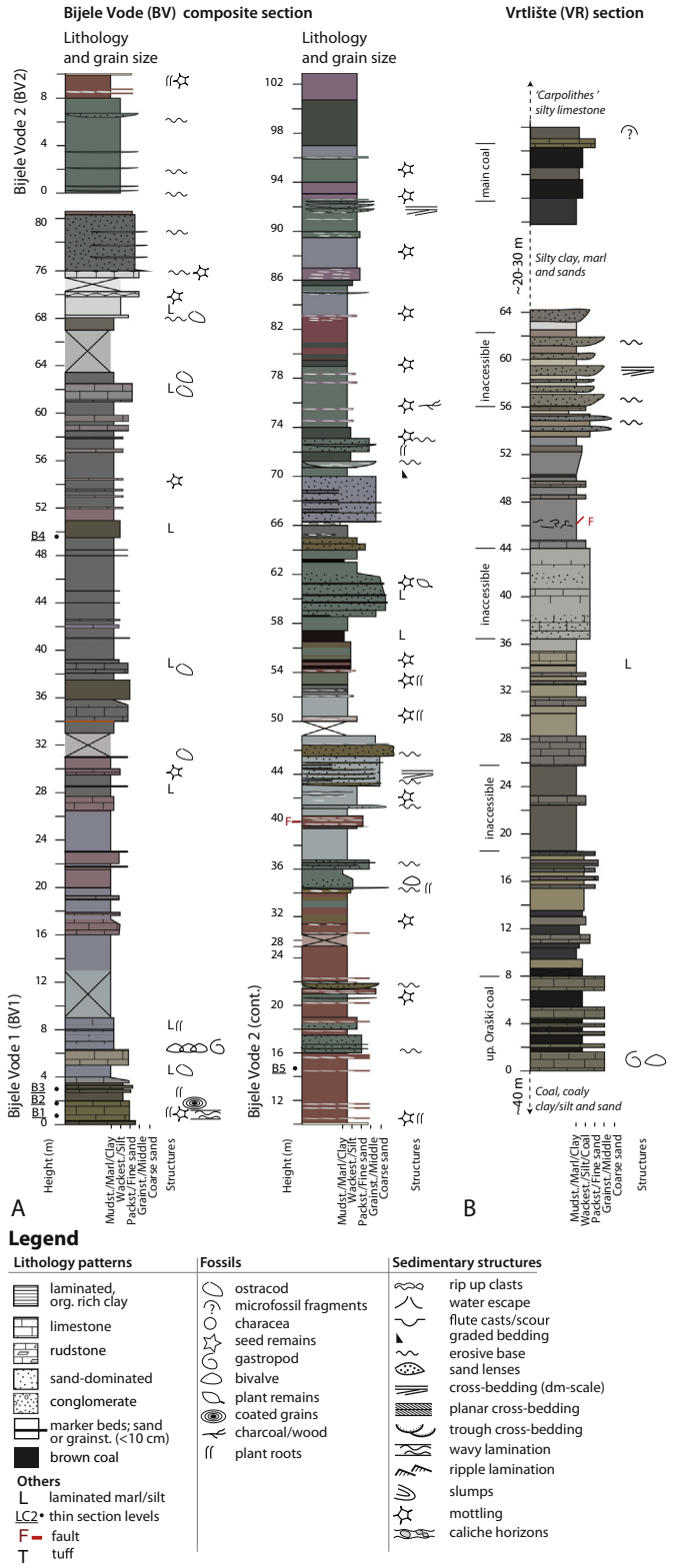


**Fig. 4.** Oligo-Miocene sections. Stratigraphic representation of the studied succession in Bijele Vode (A) and Vrtlište (B). The sections correlate with the following units of Milojević (1964) and Muftić (1965), respectively: BV with TRS 1d-2a$_1$ and Unit 2–3, VR with TRS 2a$_2$ and Unit 4. The gap between BV 1 and BV2 is ~5–20 m. The legend is valid for all figures with stratigraphic logs in this manuscript. Colors resemble the observed sediment colors in the field.

characterized by green, red-violet, yellow and gray mottled clays and silts with patches of caliche, all typical for paleosoil formation (Fig. 7G–I). Channel-like bodies of (greenish) medium to coarse sand with floating gravel and channel lags (pebble and cobble-size) are common as well. Individual channels are max. 1.5 m high and up to 25 m wide. Some sands show dm/cm-scale cross-bedding (e.g., level 44 m, BV2). Most grains are poorly sorted and mainly sub-angular. Articulated unionid shells (10 cm) are present in the green sands (Table 1). Around 56 m, some cm-scale coal intervals are present as well. Fragments of radiolarian chert, black chert, greenish grains of weathered serpentinite or diabase and quartzite can be recognized in the gravelly sandstones.

These observations suggest that at time of deposition in BV2, the area was probably covered by a flood plain, a frequently wetted area where soil formation happens in overbank deposits and lignite may form in shallow bogs (e.g., Miall, 1996). The red-purple colors of the paleosoils are the result of oxygenation of ferruginous material. This process takes place when sediments are oxygenated for a significant period of time, such as in subtropical arid climates (Bown and Kraus, 1987; Stow, 2005). Red brown colors signify well drained soils ($Fe^{3+}$) and pale (gray) color mark poorly drained soils with less oxygen ($Fe^{2+}$) (Atabey et al., 1998; Roberts, 2015). The red color, caused by hematite pigment, at places changed to green, gray or even white through secondary alteration (leaching) by passing ground water. The green color is most common in medium-coarse sands, where it could either reflect the high amount of green grains from the nearby ophiolite complex or point to recent leaching processes that altered the original color.

Most sands represent periods when a side channel or the main channel of the river is cutting into the flood plain (Miall, 1996). After filling up a channel, the top layer desiccates and the soil forming process starts again forming another paleosurface (Fig. 7). The unionid shells are characteristic for fluvial and shallow littoral lake settings (Welter-Schultes, 2012). Poor sorting and (sub-)angular grains in most sands point to a nearby source area.

The black chert fragments and green-gray grains are sourced from the Western Vardar Ophiolite complex and mélange (Schmid et al., 2008). The radiolarite, gray chert and quartzite fragments could derive from the same complex, but might also originate from the Bosnian Flysch nappe, which bears clastic material derived from the overriding ophiolites (Vranduk Fm.) and micritic limestones, red/gray shales and carbonatic mass flow deposits derived mainly from the High-Kars Unit (Ugar Fm.) (Hrvatović, 2006; Jovanović et al., 1971; Mikes et al., 2008; Sofilj and Živanović, 1971; Živanović et al., 1967).

### 4.1.2. *Vrtlište mine area*

The sediments in the Vrtlište section (~100 m) are dominated by the brown coal package of the "Orasi" coal, existing of shiny and pale brown coal layers (0.2–2 m) with organic-rich gray marl, limestone and silt interbeds (Fig. 4B). The total thickness of the Orasi coal package in VR ranges between ~7 and 20 m. The overlying sequence is laterally very variable. In the logged section it grades from dominantly dark gray (silty) carbonates to cross-bedded, channel-like sand and silts (Fig. 4B). In other parts of VR, the Orasi seam is directly overlain by these sands (Džindo, 2013). The stratigraphically younger "main coal seam" in the mine ranges from 2 to 5 m in thickness, and appears as layer or a two-fold coal seam separated by dark gray clay (Džindo, 2013). The Orasi coal package thickens towards the NE (Muftić, 1965), while the thinner main coal layer thickens towards the SW basin margin (Džindo, 2013; Milojević, 1964) (Fig. 2A). The thickest most resistant coal beds in VR are alternating with packstone lenses, that are regularly pinching out. Microanalysis shows two distinct laminae; one is mottled micrite full of organic matter, the other is packstone made of recrystallized allochems with bioturbation (Suppl. Mat. A). Both layers include recrystallized ostracod and mollusk remains, fossil fruit remains, and most likely immature plant crusts. Numerous shells of minute *Prososthenia* sp. and rare *Pisidium* sp. were encountered in limestones in the basal coal series

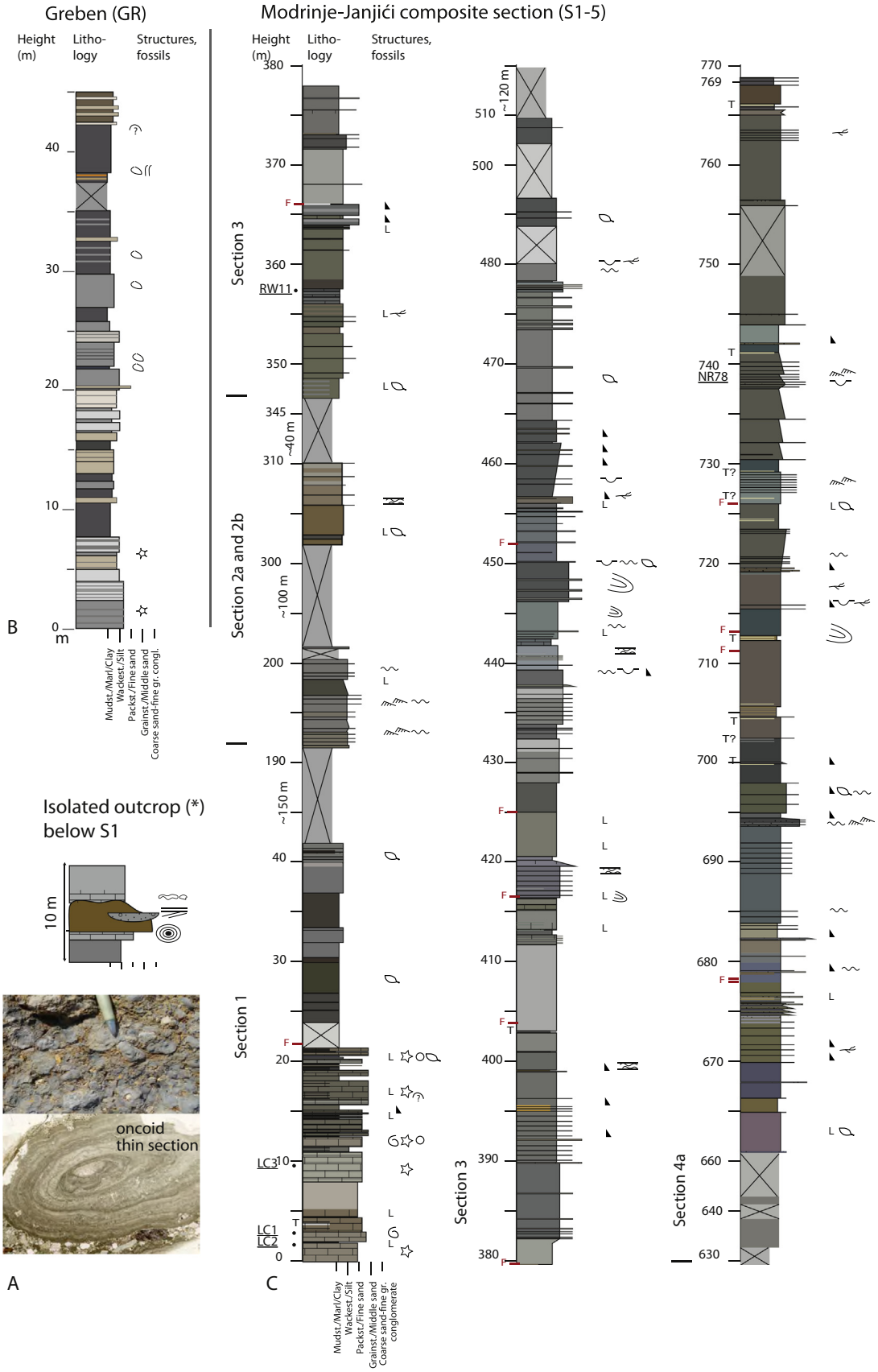


**Fig. 5.** Main lake phase sections. Stratigraphic columns of the studied intervals of the lower-middle Miocene basin phase including the oncoid sands (A), Greben mine (B) and Modrinje-Janjići composite (C) with partial sections 1 to 5. The sections correlate with following units of Milojević (1964) and Muftić (1965) - GR with TRS $2a_3$–2b and Unit 6 (*Glyptostrobus* Zone), Modrinje-Janjići S1 probably with TRS $2a_3$-2b and Unit 5–6, S2–S4 with TRS 2b and Unit 7 (*Delminiella* Zone) and S4–5 with TRS 2c and Unit 8 (Lašva Fm). (A) A typical sequence and photographs (oncoids) for the facies found below S1. Colors resemble the observed sediment colors in the field. See Fig. 4 for symbol legend.

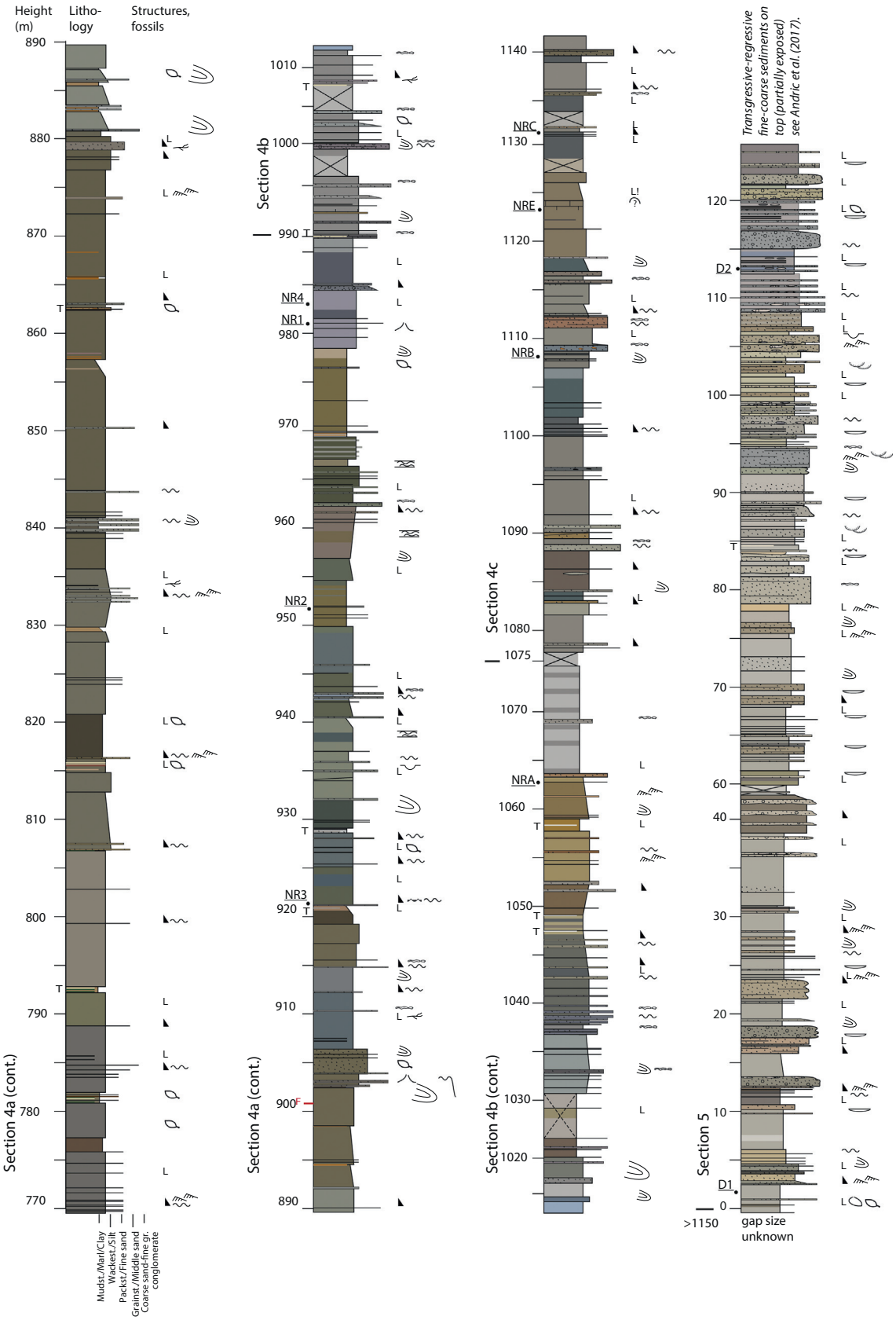


**Fig. 5.** (*continued*)

**Table 1**
Sample locations and identified species of mollusks and ostracods. + = present, ++ = abundantly present.

| Samples | R1a (Sept, 2014) | R1b (Sept 2014) | R2 (Oct 2014) | BV2 (Sept, 2014) | VR - level 3.2 (Oct, 2014) | GR - base (2007, 2015) | GR - top (2007, 2015) | GR1 (Oct 2014) | M1/D4 (Oct, 2015) | Sopotnica (Sept, 2014) | P1 (Oct 2014) | C1 (Oct 2014) | "Unit 3" | "Unit 7" |
|---|---|---|---|---|---|---|---|---|---|---|---|---|---|---|
| **Section/locality** | Bijele Vode 1 - 7 m | Bijele Vode 1 - 7.1 m | Bijele Vode 1 - 61 m | Bijele Vode 2 - 34 m | Vrtliste | Greben | Greben | Greben - 21.5 m | Between S1 and S2a | Sopotnica village (parallel to base S4a) | Poriječani (2M2 - "transitional zone" unit) | Smrsnica (basal Lašva unit) | lower coal seam group (Muftić, 1965) | *Velutinopsis* unit (Muftić, 1965) |
| **Lithology / notes** | Wackestone | Gray brown wackestone | Dark gray silty marlstone | Gray-green sandstone | Silty limestone | Mudstone/ wackestone | Silty marlstone | Gray silty marl | Platy marlstone | Silty marl with fine grained calcarenites/sandstones | Light brown, resistant laminated sandy marl | Gray silty marls | | |
| **GPS data** | 44.160529°, 18.110819° | 44.160529°, 18.110819° | 44.161607°, 18.110390° | 44.161943°, 18.108763° | 44.138353°, 18.094016° | 44.139028°, 18.121835° | 44.139206°, 18.123272° | 44.138770°, 18.122008° | 44.140775°, 18.014776° | 44.116721°, 18.000274° | 44.044853°, 18.169827° | 44.032806°, 18.186866° | | |
| **Mollusks** | | | | | | | | | | | | | | |
| *Radix* aff. *dilatata* (Noulet) | | | | | | | | | | | | | + | |
| *Delminiella soklic* | | | | | | | | | | + | | | | + |
| *Clivunella katzeri* | | | | | | | | | | | | | + | + |
| *Prososthenia* sp. | | | | | ++ | | | | (?) | | | | | |
| Unionidae *(gen et sp. Indet,* | | | | + | | | | | | | | | | |
| *Pisidium* sp. | ++ | | | | + | + | + | | | | | | | |
| **Ostracods** | | | | | | | | | | | | | | |
| *? Aurila sp.* | | | | | | | | | | | + | | | |
| *? Cyprideis* sp. | | | | | | | | | | | + | | | |
| ? *Leptocythere* sp. | | | | | | | | | | | | + | | |
| *Amplocypris* sp. | | + | | | | | | | | | ++ | + | | |
| *Candona sp.* | | | + | | | | | | | | ++ | + | | |
| *Candona* (*Pontoniella*) sp. | + | + | | | | | | ++ | | | + | ++ | | |
| *Candona* (*Camptocypria*) sp. | | | | | | | | | | | + | ++ | | |
| *Candona* ex gr. *candida* | ++ | | | | | | | + | | | | | | |
| *Candonopsis* sp. | + | + | | | | | | + | | | | + | | |
| *Cyclocypris* sp. | | | | | | | | + | | | | | | |
| *Cypria* sp. | | | + | | | | | + | | | | | | |
| *Cypridopsis biplanata* | | | ++ | | | | | | | | | | | |
| *Fabaeformiscandona* sp. | + | + | | | | | | + | | | + | ++ | | |
| *Herpetocypris* sp. | | | + | | | | | | | | + | ++ | | |
| *Ilyocypris sp.* | | | | | | | | + | | | | | | |
| *Limnocythere* sp. | | + | | | | | | | | | | + | | |
| *Limnocythere* sp. 1. | | | | | | | | ++ | | | | | | |
| *Limnocythere* sp. 2 | | | | | | | | + | | | | | | |
| *Moenocypris* sp. | | | ++ | | | | | | | | | | | |
| Ostracoda sp. nov. | | | | | | | | ++ | | | | | | |
| *Paralimnocythere* sp. | + | | | | | | | + | | | | | | |
| *Pseudocandona* sp. | | | | | | | | | | | | + | | |
| **Flora** | | | | | | | | | | | | | | |
| *Glyptostrobus europeus* (flora) | | | | | | | ++ | | | | | | | |

**Table 2**
Correlation of the lithostratigraphic units of the central Sarajevo-Zenica basin.

| Correlation of the lithostratigraphic units of the central Sarajevo-Zenica basin | | | | | | |
|---|---|---|---|---|---|---|
| Fig. 2 | Milojević, 1964 | | | Muftić, 1965 | | |
| IV | $^{1}M_{3}$ | Koševo series | | 9 | Sandstone unit | |
| III | $M_{2-3}$ | Lašva series | | 8 | Limestone and sandstone unit | |
| | $^{2}M_{2}$ | Transitional zone | | 7 | *Velutinopsis unit* | |
| | $^{1}M_{2}$ | Roof zone | Main coal zone | 6 | *Glyptostrobus unit* | |
| II | | | | 5 | Roof coal seam | |
| | | | | | *Carpolithes limestone* | |
| | $M_{1-2}$ | Main zone | | 4 | Upper coal seam group | Main coal seam |
| | | | | | | |
| | | | | | | Orasi coal seam |
| | $M_{1}$ | Floor zone | | 3 | Lower coal seam group | |
| | $^{4}$Ol,M | Tufaceous bituminous limestone | | 2 | Close floor bed group | |
| I | $^{3}$Ol,M | Red series | | 1 | Basal bed group | |
| | $^{2}$Ol,M | Platy limestone | | | | |
| | | Košćani coal seam | | | | |
| | $^{1}$Ol,M | Basal zone | | | | |

of VR (Fig. 6P–R, Table 1).

The limestone lenses within the coal-dominated successions likely represent calm ponds within a swamp-to-palustrine environment dominated by the influx of organic matter. Transport of the organic material was very short, in agreement with the immature plant crusts found in the limestones. The light-dark laminae show that poor and well-oxygenated periods alternated. The masses of the hydrobiid *Prososthenia* snails indicate shallow littoral conditions within well-oxygenated periods. The poor oxygenated periods are reflected by a relatively high sulfur content (3–5%) detected in Miocene coal deposits in the basin in general (Milojević, 1964). Such high sulfur coals are indicative for anoxic and alkaline environments with a high supply of sulfur (Chou, 2012; Mandic et al., 2009). The sulfur might originate from a wide range of processes, such as fluids circulating along the fault plane, a high bacterial activity or input of volcanic material into the basin (Cohen, 2003c; Petrascheck, 1952; Taylor et al., 1998).

### 4.2. The lower-middle Miocene lacustrine sediments

One typical facies is present at the base of the lower-middle Miocene lacustrine succession, but the studied isolated outcrop is not part of a section. It lies stratigraphically beneath S1 (marked by * in Fig. 2B), and similar sediments were found from top of the VR section. It comprises silty marl-to-silt with yellow-brown calcareous and siliciclastic sand bodies with oncoids, and frequent cm-scale ripples and cross-bedding (Fig. 5A). Microanalysis of the oncoid sands shows that it is quartz-dominated with subordinate Cretaceous phytoplankton-bearing limestone clasts and phyllite. This facies, with oncoids and cross-beds, were most probably deposited in a shallow dynamic shore environment influenced by wind, waves and land-derived clastic input (Peryt, 1983). The Cretaceous phytoplankton is likely derived from the Ugar Fm (Bosnian Flysch).

#### 4.2.1. Greben section

The lower part of the Greben section (45 m) is dominated by light and dark gray wackestones with omnipresent dispersed organic matter on their bedding planes (Fig. 5). One dark-gray silty marlstone horizon stands out around 10 m stratigraphic level (photo in Fig. 3). A gradual transition to darker colors and finer-grained sediments takes place in the upper fraction (> 20 m). In contrast to the underlying carbonates, this part of the section is rich in ostracods, and contains scattered microgastropod shells of the hydrobiid *Prososthenia* and imprints of plants such as the conifer *Glyptostrobus europaeus* (Fig. 6, Table 1) (see Pantić

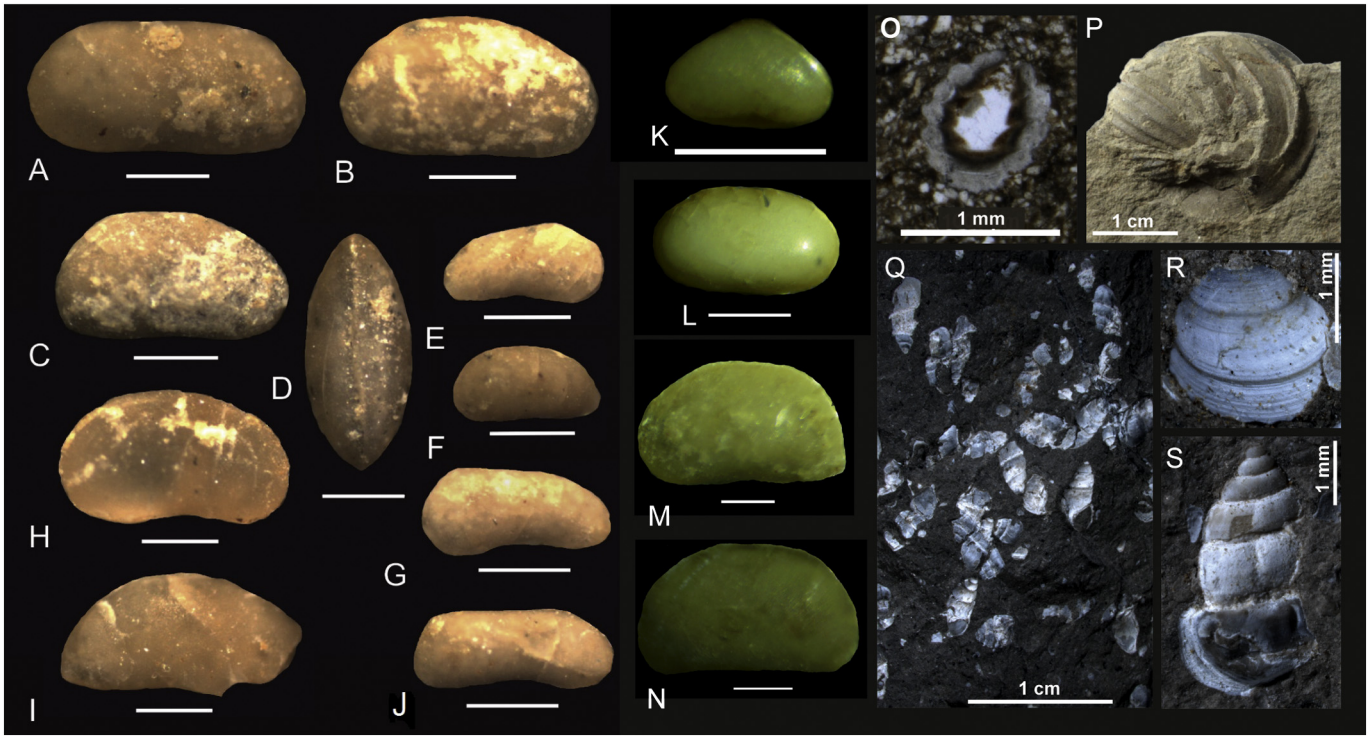


**Fig. 6.** Fossils – localities are displayed in Table 1. Ostracods - Sample C1: (A,D) *Herpetocypris* sp. (A - left carapace; D - dorsal view); (B,C) *Amplocypris* sp., right valve; (E,F) *Candona* (*Pontoniella*) sp. (E - right valve, F - left valve); (G,J) *Fabaeformiscandona* sp. (G - right c.; J - right c. [compressed]); (H) *Candonopsis* sp., right c.; (I) *Candona* sp., right c. Sample RI2: (K) *Cypridopsis biplanata* Straub, sensu Sokač (left c.); (L) *Moenocypris* sp. (left c.). Sample P1: (M) *Candona* sp. (left c.); (N) *Amplocypris* sp. (left c.). (O) Characea in thin section (slide LC2, S2). Mollusks - (P) *Delminiella* cf. *soklici* (Sopotnica village, ~base S4); (Q) Accumulation of *Prososthenia* sp. and (R) *Pisidium* sp. (VR); (T) *Prososthenia* sp. (VR).

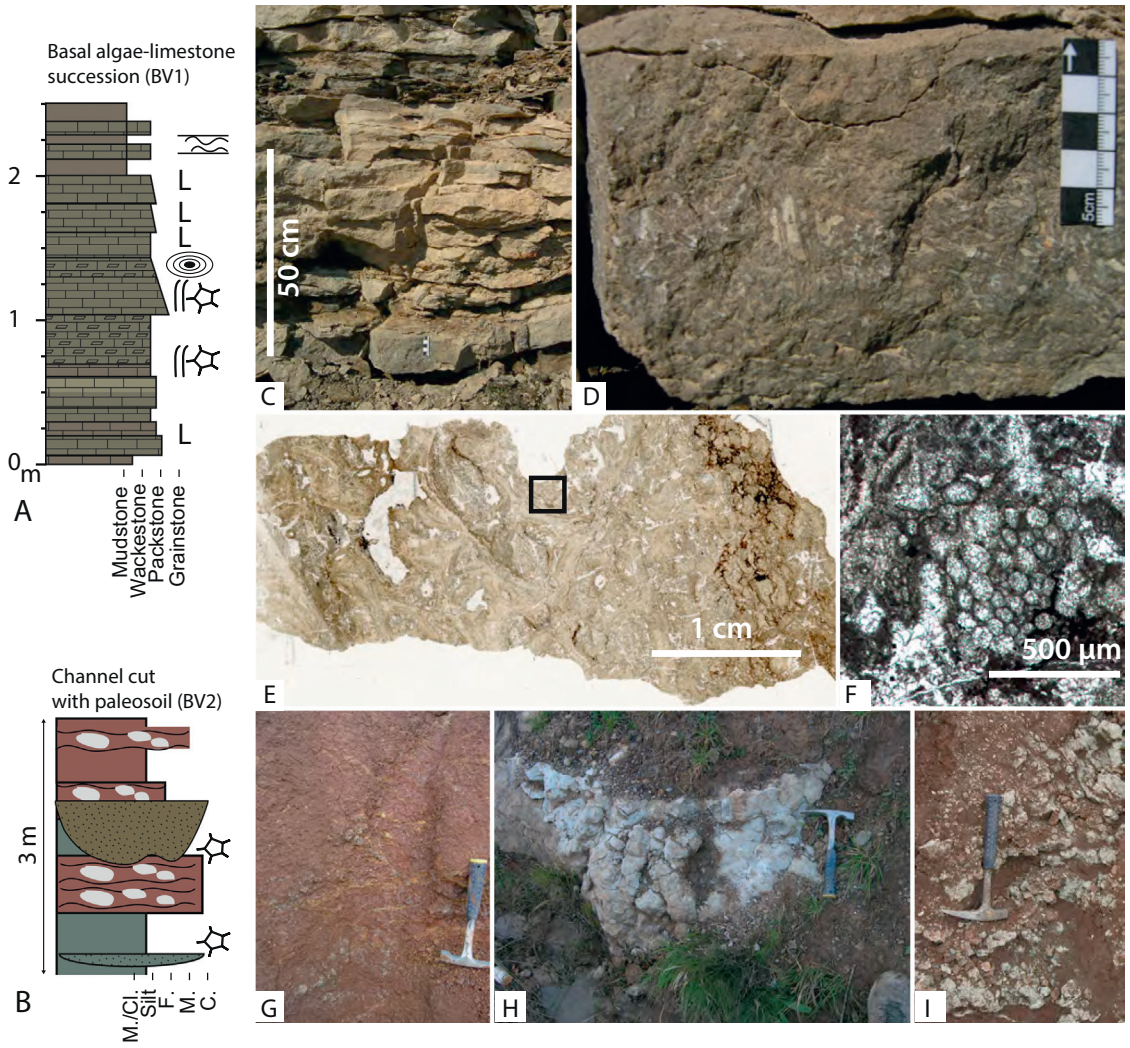


**Fig. 7.** Bijele Vode highlights. Typical stratigraphic sequences (A–B) with macro- and microscopic images of sedimentological details from the Bijele Vode section. (C) Microbialite pack-to-rudstone bed at the base of BV1 with a rudstone depicted with increasing magnification (C–F), including a honey comb structure (F). (G) typical red mottled continental clay, (H) brecciated limestone fragments in a carbonate matrix, (I) caliche in red silt. See supplementary material B for additional thin slide photographs. (For interpretation of the references to color in this figure legend, the reader is referred to the web version of this article.)

et al., 1966 for more plant fossils). The studied ostracod level at 21 m (sample GR1) contains a diverse assemblage, dominated by elongated candonids and small *Limnocytherids,* and *Ilyocypris* (Fig. 6, Table 1). Some of the taxa have tiny, more or less transparent carapaces (e.g., *Pontoniella, Cypria, Cyclocypris*).

The ostracod assemblages generally indicate freshwater-oligohaline conditions (Lorenschat et al., 2014; Meisch, 2000) (Suppl. mat. A). The fragile carapaces suggest the presence of only a small amount of dissolved salts, and a low-energy environment with relatively calm water (Rundić, 1998; Sant et al., 2018). In the existing stratigraphic scheme, the Greben section corresponds to the *Glyptostrobus* limestone and overlying marls of the Transitional Zone (TRS2$a_3$-b by Milojević, 1964). In that respect, it should correlate to the central part of S1 of the Modrinje-Janjići section, perhaps to the interval ~21 m that might be missing due to an oblique strike-slip fault (Figs. 3, 5B). Alternatively, the Greben sediments could be a distal equivalent of the limestones in S1.

#### 4.2.2. The Modrinje-Janjići composite section

The base of the overlying Modrinje-Janjići section (S1: 0–22 m) is dominated by brown-gray organic rich limestones (2–50 cm) intercalated by thinly bedded dark-brown to black silt, clayey marl and brown coal (1–50 cm) (Fig. 5). The carbonates contain recrystallized fragments of characea, fruits, plants (weed) and ostracods, and poorly preserved hydrobiid snails, like *Fossarulus tricarinatus* and operculi of *Bithynia* (Figs. 6, 8A,B). The silty packstones and grainstones have characteristic gray to dark gray laminations. Bioturbation is concentrated in the lighter colored lamina, whereas the darker parts are almost barren. Above 22 m, the resistant limestones in S1 suddenly make way for dark-gray and brown clayey marls (30–60 cm thick) alternating with some 10 cm-thick intercalations of red-gray weathered marlstones.

The charaphyte-limestones ("*Carpolithes*" limestone sensu Milojević, 1964) typically reflect very shallow water (< ~10 m). The laminae resulted from alternating oxygen levels, which might be related to seasonal variation or climate-variability. The shift to marls indicates a deepening from a shallow to perennial lake environment which is registered in the whole basin (Muftić, 1965). Actually, this change is not a sharp line in basin stratigraphy, but rather a transitional interval. In S1 the shift in lithology seems very abrupt because it is amplified by a post-sedimentary strike-slip fault (Fig. 5). Like pointed out in 3.4.1, a part of the stratigraphy bearing the *Glyptostrobus* limestones (GR) might be missing at this level.

In S2, the first thin (1–5 cm) sands appear, some with an irregular base, horizontal laminae, or traces of cross-bedding (or ripples). Between 300 and 365 m, brown-green clayey marls with some typical

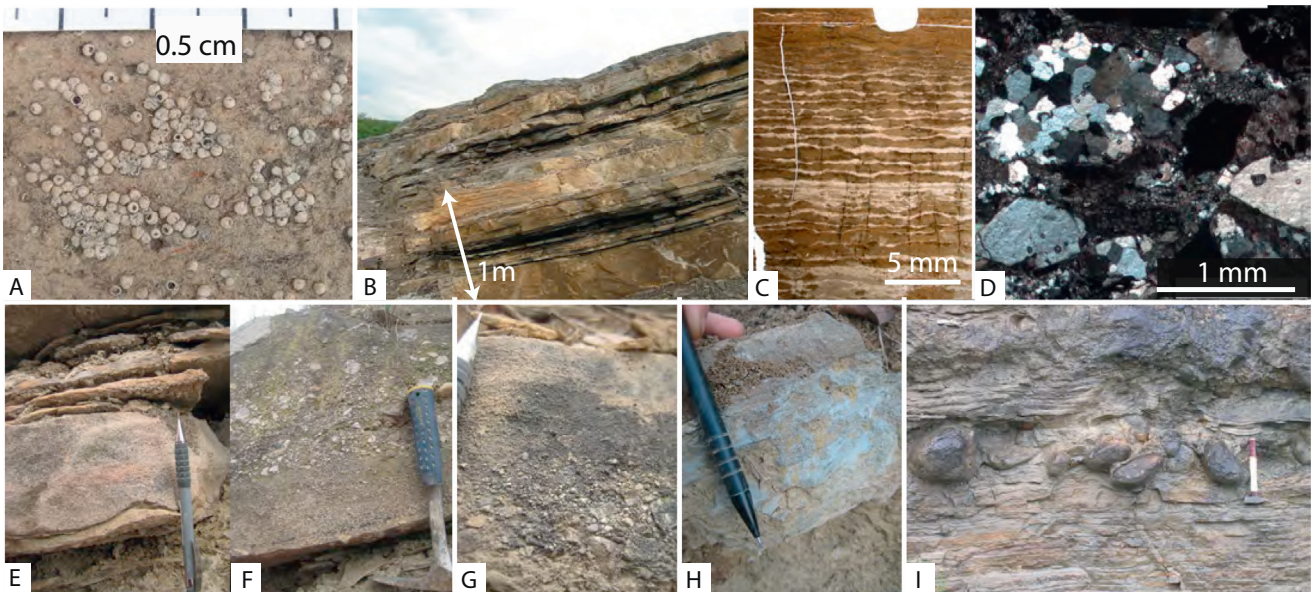


**Fig. 8.** Modrinje-Janjići highlights. Macro- and microscopic images of sedimentological details from the Modrinje-Janjići composite section. (A) Charaphyte fossils in a silty packstone (S1, level 11.5 m), (B) Limestone - coal/organic rich silt alternations (S1, interval 11–15 m) (C) Wavy lamination on a microscale in a mudstone (S3, level 419 m), (D) Typical deformed quartz grain and feldspars in a coarse sand (S4, level 982.5 m). (E) Turbiditic medium grained sand to silt with erosive base, grading and poorly developed ripple lamination on top (S5, level 13 m), (F) Amalgamated sand to matrix-supported conglomerate (S5, 14 m), (G) Fining upwards in a sand level in S5 (level 3 m); Bosnian schist elements are obvious, (H) Typical slumped layer with a chaotic mixture of blue-gray silt with coarse sand (S4-b, level 990 m), (I). Semi-rounded boulders in channel lag surrounded by thinly bedded fine sand (S5, level 93 m). See supplementary material B for additional thin slide photographs. (For interpretation of the references to color in this figure legend, the reader is referred to the web version of this article.)

mm-scale laminated intervals of silty clays full of plant remains exist. Above 365 m (S3), silty marl dominates, alternating with thin (1–10 cm) non-erosive calcarenites or fine-grained quartz-arenites. Most silty marls and sands are laminated on a microscale with organic matter in horizontal or wavy lamina (Fig. 8C). Many sands are immature, reflecting short transport and fast burial. The calcarenites and fine sands are a mix of calcareous grains (some are dolomite) and deformed quartz grains with rare biotite remains. Upwards in the section (S4b–c, S5), medium-coarse sands appear more frequently. They show normal grading and regularly contain erosive bases and flute casts with gravel or pebbles (Fig. 8E). Section 4b–c has many very fine to very coarse chaotic sandstones (5–50 cm thick) with sand of different grain sizes in lenses, gravel and rip-up clasts (Fig. 8H).

S5 (up to ~78 m) is dominated by laminated silty marl to marly siltstone perturbed by (mostly) non-erosive fine and medium qz-sandstones or clast-to-matrix supported conglomerates of irregular thickness (2–5 cm). Above, sandstone dominates, and most sand bodies are wedging or lense-shaped (Fig. 5). The average clast size of the conglomerates is pebbles to cobbles, yet even boulders appear in the uppermost 40 m. The sand and conglomerate bodies, including elements of turbiditic flows (fining upwards, cross-bedding, planar lamination etc.) and cohesionless debris flows (clast-supported conglomerate, planar base etc., such as the chaotic sand beds in S4b-c), have been described in detail by Andrić et al. (2017) (Fig. 8F–I). The top is dominated by conglomerates (top of S5). Typical features include wedging sand bodies forming trough cross-bedding, cohesive debris flows and alluvial channels (Table 1 in Andrić et al., 2017). On top of the conglomerates follow several coarsening upwards packages of lacustrine marls to conglomerates. In fact, the succession directly overlying S5 is fining upwards in general (Andrić et al., 2017) (Fig. 3).

Dispersed organic matter is omnipresent in S2–5 of the Modrinje-Janjići composite section. Leave imprints on bedding surfaces (e.g., *Daphnogene* [=*Cinnamomum*]) and coal pockets are common in both the marls and the sands. Especially S4 is full of mm-scale tuff intercalations. Slump intervals occur frequently, most importantly at 712, 885 and 930 m. Several intervals with rhythmic alternations of silty marl and fine sands occur in S3 and 4a (e.g., 417–420 m; 690–692 m). Some fining upwards trends from conglomerate or sand to marl are distinguished at 0.1 to 10 m-scales (e.g., 730–743 m), whereas on a larger scale packages seem to be coarsening and thickening upwards (e.g., 420–440 m, 950–966 m). Coarsening upwards packages (5–10 m) are most prominent in the lowermost 50 m of S5.

The silty lacustrine marls represent the background sedimentation that gets increasingly perturbed by siliciclastic material. The thin laminated siltstones and calcarenites are most likely the distal equivalents of incoming turbidity flows and waning floods from the active margin of the basin (Facies Unit *Te* in Andrić et al., 2017). Many sands in S3–5 are most likely poorly developed turbidites and non-cohesive debris flows (Fig. 8H). Their presence is in agreement with a syn-tectonic setting and a nearby low gradient basin slope. The coarsening of the lithologies with time reflects the progradation of the delta front towards the basin center (Andrić et al., 2017). The conglomerate-dominated top of S5 marks a point where sediment input exceeded accommodation space, the basin got filled, and the environment prograded from delta slope to an alluvial fan setting (Andrić et al., 2017).

Fossils are very rare in the majority of the Modrinje-Janjići section (S2–5). One *Delminiella* cf. *soklici* mollusk was found in a locality parallel to the base of S4 (Fig. 6P). Ostracods were only encountered at the base of S5. Two samples (P1 and C1) from the SSE of the Sarajevo-Zenica Basin with similar facies as in S4-c yielded ostracods. P1 is dominated by large (1.5–2.2 mm) *Amplocypris* and *Candona*, whereas in C1 large *Herpetocypris, Fabaeformiscandona, Candonopsis and Camptocypria* are most common (Fig. 6). In the latter almost all carapaces are recrystallized and Fe, S and Mn accumulations are prevailing.

The general scarceness of fossils and the presence of *Delminiella* snails, are associated with a deeper water setting than for the underlying limestones (S1, GR), suggesting a profundal setting in an open perennial lake (Kochansky-Devidé and Slišković, 1972). The ostracod assemblages generally have a freshwater - oligohaline character. Some species can withstand higher salinities too (e.g., *Amplocypris* and *Cyprideis*) (Gross, 2008; Rundic, 2006). The occurrence of relatively large ostracod specimens suggests shallow-water conditions with more

dissolved salts and increased water energy compared to the setting recorded at the base of the Greben section (Rundić, 1998). The re-appearance of ostracods in the basal part of S5 concurs with the re-appearance of shallower lacustrine conditions.

The first microscopic evidence of input of biotite-schists and dolomitic limestones of the Mid-Bosnian Schist mountains (Jovanović et al., 1971) is recorded at 358 m (Fig. 5). Sands and conglomerates of S3–4 commonly include large grains or pebbles of deformed quartz, biotite, muscovite, and limestone clasts, and subordinate feldspar (plagioclase), chert and garnet (Fig. 8D). Lithoclasts in coarse sands include chlorite-biotite-schists, rhyolite fragments, dolomite and dolomitic limestones. The same elements are clearly macroscopically visible in gravel and pebbles, showing a dominant provenance of the Mid-Bosnian Schist Mountains. In contrast, the largest pebbles and cobbles in S5 contain dominantly gray limestones and cherts typical for the Ugar Fm of the Bosnian Flysch Unit (e.g., levels 14, 37, 97 m) (Mikes et al., 2008). The presence of mainly Ugar flysch pebbles and cobbles in S5 shows that variation in the type of clasts is highly dependent on the location within the basin; S5 is positioned to the north of the basin, where Ugar flysch rocks are presently exposed (Fig. 2).

### 4.3. Biostratigraphic implications

The studied ostracod assemblages found in all studied samples of the Sarajevo-Zenica basin share very few taxa with other DLS records, mostly assigned to late early to middle Miocene localities (Jurišić-Polšak et al., 1993; Krstić et al., 2009; Sokač, 1979; Sokač and Krstić, 1987). A few taxa, a.o. *Pseudocandona* sp., *Amplocypris* sp., *Herpetocypris* sp., *Cypridopsis biplanata* and *Fabaeformiscandona* sp., are similar to those from the middle Miocene locality Sadovi (Požega basin) in NW Croatia (Hajek-Tadesse et al., 2009; Pavelić and Kovačić, 2018). In the Gacko Basin, similarities are limited to the taxa *Cypridopsis biplanata* and juvenile *candonids* (Krstić et al., 2009). Many species seem to have a wide stratigraphic range and low biostratigraphic significance, such as *Amplocypris*, which we found in the palustrine "Oligo-Miocene" limestones (BV1) and also in the marls of the lower-middle Miocene part of the Sarajevo-Zenica Basin. It also occurs throughout the entire lower-middle Miocene lacustrine infill of the Livno Basin (Muftić and Luburić, 1963). In general, the ostracods have Miocene affinities, and no typical Oligocene ostracods were found in Bijele Vode.

Note that a detailed account of Miocene ostracods for the Dinarides is lacking. The use of outdated or local genus/species names in old (pre-1970) reports (e.g., Brady and Norman, 1889; Mehes, 1907; Müller, 1900) complicates comparison of these ostracods to those of later studies (e.g., Krstić, 1972; Meisch, 2000).

Muftić (1965) and Kochansky-Devidé and Slišković (1972, 1978) described the distribution of the clivunellid (*Clivunella* and *Delminiella*) gastropods and dreissenid ("*Congeria*") bivalves in the Sarajevo-Zenica Basin. More specifically, Muftić (1965) reported the lowermost occurrence (LO) of the gastropod *Clivunella katzeri* in facies correlating with the BV section, and the LO of the gastropod *Fossarulus* spp. in facies correlating with the VR section (Table 1). The clivunellid peak diversity occurred in the carbonates of the *Glyptostrobus* Zone (sensu Muftić, 1965; e.g., GR section) contributed by *C. elliptica*, *Delminiella excentrica* and *D. soklici*. The ultimate clivunellid occurrence in the succession was recorded in the *Delminiella* Zone (sensu Muftić, 1965; ~S2). The LO of the dreissenid bivalves was recorded in the *Glyptostrobus* Zone with the three species "*Congeria*" *pilari*, "*C.*" *zoisi*, and "*C.*" *obliqua*. The diversity maximum occurred in the *Delminiella* Zone bearing "*Congeria*" *pilari*, "*C.*" *zoisi*, "*C.*" *soklici*, "*C.*" *sliskovici*, "*C.*" *socialis pennata*, "*C.*" *novica*, "*C.*" *venusta*, and "*C.*" *jadrovi*.

The mollusk findings of this study coincide well with these previous data. The presence of *Prososthenia* sp. in the base of VR enriches the data set, and the LO of *Delminiella* aff. *soklici* in a section parallel to the base of S4 (Sopotnica village) yields valuable biostratigraphic information for the Sarajevo-Basin Basin infill (Table 1).

The mollusk distribution shows that the endemic mollusk fauna of the Illyrian Bioprovince (DLS and southern Pannonian Basin) is present throughout the basin (Mandic et al., 2012). The lowermost occurrence of this fauna is lower Miocene; their oldest occurrence is $^{40}Ar/^{39}Ar$-dated ~18 Ma (de Leeuw et al., 2010, 2012; Mandic et al., 2012). The clivunnelid gastropods are restricted to the lower Miocene and, hence, mark the early phase in the evolution of the DLS fauna (de Leeuw et al., 2011b). Their presence up to the base of S4 indicates an early Miocene age of the underlying succession. This age range is supported by the absence of middle Miocene dreissenid species, such as *Illyricocongeria drvarensis*, *I. fritzi* or *I. aletici* in that part of the section (de Leeuw et al., 2010, 2011b, 2012; Mandic et al., 2011; Neubauer et al., 2015c). An ecological cause of their absence is ruled out, because many other species of dreissenid bivalves are present in that interval as referred to in the text above.

One additional biostratigraphic constraint for correlation of the magnetostratigraphy to the Global Polarity Time Scale (GPTS; Hilgen et al., 2012) is provided by the fossil *Deinotherium bavaricum* from the main coal layer at the base of the lower-middle Miocene lacustrine phase (Milojković, 1929) (Fig. 11). This elephantoid is part of a larger group called proboscideans which migrated from Asia and arrived in Europe during the early Miocene. The maximum age for the primitive form of *D. bavaricum,* which is in some cases named *D. cuvieri* (e.g., Böhme et al., 2012), in SE Europe is ~18.4 Ma (K/Ar-data, Lesvos; Koufos et al., 2003). The oldest proboscideans appeared in Central Europe after 17.5 Ma ($^{40}Ar/^{39}Ar$-data, N. Hungary; Pálfy et al., 2007). In Germany, *D. cuvieri* occurred from 18.1 to 17.5 and *P. bavaricum* occurred from ~15.7 to 13.2 Ma (Mainz Basin, Böhme et al., 2012). An even younger *Deinotherium* first occurrence (17.6 Ma) and older last occurrence (12.7 Ma) was indicated for the same region by Pickford and Pourabrishami (2013). In the DLS, a proboscidean fossil was dated at 17.0 Ma ($^{40}Ar/^{39}Ar$-data, Livno Basin; de Leeuw et al., 2011b). Summarizing, the sediments overlying the main coal layer should be younger than ~18.4 Ma.

Regional correlations between DLS basins based on plant stratigraphy are often inconsistent (e.g., Pantić et al., 1966). For example, the Orasi coal seam in VR (lower Miocene) was correlated with the upper Oligocene coals in Banovići and Ugljevik (de Leeuw et al., 2011a; Pezelj et al., 2013), but also with the lower Miocene floral assemblage from Livno (~17 Ma; de Leeuw et al., 2011b). The *Glyptostrobus* Zone in the Miocene Sarajevo-Zenica Basin (lower Miocene) bears flora comparative to the middle Miocene one from Lake Popovac in Serbia (Sant et al., 2018). These conflicting ages suggests that the recorded plant distribution patterns depend primarily on paleoecological constraints, making regional plant stratigraphy often unsuitable for solving regional correlation problems. Therefore, pollen-based stratigraphy should be treated with care.

## 5. Magnetostratigraphy

### 5.1. Paleomagnetic and rock magnetic lab procedures

All paleomagnetic and rock magnetic measurements were carried out at Paleomagnetic Laboratory Fort Hoofddijk at Utrecht University. Prior to the demagnetization experiments, the magnetic susceptibility per mass was determined for all samples using an Agico MFK1 Kappabridge at field strength of 200 A/m and a frequency of 976 Hz. Moreover, a representative fraction of 33 samples was selected for stepwise Isothermal Remanent Magnetization (IRM) acquisition using a 2G Pulser in line with an automated system (Mullender et al., 2016). Sixty IRM steps with a peak field of 700 mT were applied. Small powdered amounts (~200 mg) of 28 representative specimens were additionally used for thermomagnetic experiments using a modified horizontal translation type Curie balance (noise level $5 \times 10^{-9}$ A m$^2$) (Mullender et al., 1993). Acquisition data of the IRM was divided by mass and interpreted using the component analysis of (Heslop et al.,

2002) and Kruiver et al. (2001). The number of components has been constrained to two or three, depending on the shape of the linear acquisition plot (LAP), gradient acquisition plot (GAP) and standardized acquisition plot (SAP).

A total of 253 samples were treated with alternating field (AF) demagnetization by means of a laboratory built automated system (Mullender et al., 2016). Another group of 165 specimens were heated stepwise with 20–30 °C increments up to maximum 480 °C using a magnetically shielded ASC thermal demagnetizer. In both cases the magnetization was measured in three components at each demagnetization step with a 2G Enterprises DC Squid magnetometer (noise level: $3{\cdot}10^{-12}$ A m$^2$). The iron sulphide greigite is very common in lacustrine sediments (Sant et al., 2015; van Baak et al., 2016; Vasiliev et al., 2008). It may acquire a Gyroremanent Magnetization (GRM) during AF demagnetization in fields > 40 mT (Stephenson and Snowball, 2001). Therefore, additional field steps were taken > 25 mT and the per component demagnetization scheme of Dankers and Zijderveld (1981) was used to avoid a large GRM. Interpretation of demagnetization directions was carried out in Paleomagnetism.org (Koymans et al., 2016). Here, the linear segments at the orthogonal projection of the data (Zijderveld, 1967) were quantified with a least square method (Kirschvink, 1980; McFadden and McElhinny, 1988). Common paleomagnetic statistics, including the uncertainty of the vector fits (Fisher, 1953), the Cartesian bootstrapped function for the common true mean direction (CTMD) and reversal test (McFadden and McElhinny, 1990), the fold test (Tauxe and Watson, 1994), and the Inclination/Elongation test for compacted sediments (Tauxe and Kent, 2004) were applied via tools on the same website.

### 5.2. Rock magnetic results

An abrupt change from low to high susceptibility (av. $4.8 \times 10^{-8}$ to $2.0 \times 10^{-7}$ m$^3$/kg) is observed in S1, which coincides with an abrupt change in lithology from limestone to silty marl (Suppl. Mat. B). After this, the magnetic susceptibility in the profile is generally increasing upwards in the marls of S1–4. The values in sections 2, 4 and 5 are very similar with average values of 4.3, 5.2 and 5.3 $\times 10^{-8}$ m$^3$/kg, respectively.

The majority of the samples in the normalized IRM acquisition graph show a very steep gradient up to 100 mT (Fig. 9A). Some exceptions, such as sample NR104a and NR71.1a, have much lower gradients up to 700 mT. These samples also show specific remanent coercivity force ($B_{1/2}$) and dispersion parameter (DP) values for the dominant magnetic components fitted to the LAP, GAP and SAP curves (Suppl. Mat. C). The first and largest group (76% of all reliable specimens), has only one significant magnetic carrier in the medium field range with an average of ~80% of the total intensity. The material in the second group, including the samples with the lower gradients up to 700 mT in the normalized IRM figure, have a significant high field component (38–58% of total) besides their medium field carrier. The $B_{1/2}$ value of the medium field component varies between 31.3 and 81.3 mT, whereas the DP ranges between 0.18 and 0.34. Above ~420 m stratigraphic height it shifts towards values above 60 mT and generally low DP values (< 0.25), which could indicate the occurrence of the iron sulfide greigite. Lower remanent coercivity forces and dispersion parameters in the range 0.25–0.3 may indicate magnetite grains oxidized in variable degrees (Hüsing et al., 2009; Kruiver et al., 2001). The high field magnetic carrier has a mean $B_{1/2}$ of 913.3 mT and a DP of 0.3, and is unsaturated at 700 mT. This mineral represents hematite or goethite.

During the thermomagnetic runs, the samples behave similarly with a relatively low starting intensity < 0.02 A m$^2$/kg and a clear peak between 410 and 610 °C, reflecting the built-up of magnetite at the expense of the thermal breakdown of pyrite (Fig. 9B). Some signals are clearly not reversible between 250 and 350/400 °C, which is mainly detectable in stronger samples like in S1, where intensities are generally higher (< 0.05 A m$^2$/kg). The irreversible behavior below 400 °C is typical for an iron sulfide, in most cases greigite. The presence of pyrite, causing the large magnetite spike above 400 °C, hampers detection of primary magnetite during the thermal experiments.

In conclusion, the sedimentary rocks of the Sarajevo-Zenica Basin contain multiple magnetic carriers, with numerous samples revealing greigite and/or magnetite and in some cases also hematite is present.

### 5.3. Demagnetization results and quality

Since most of the studied material shows similar demagnetization and rock magnetic behavior, the results will be discussed together (Figs. 9, 10). A low temperature or low field component, if present, exists at least between 80 and 180 °C (Fig. 9C). In stronger samples it may reach 240 or 260 °C. The higher temperature/coercivity field component is generally stable in the temperature range 260–380/410 °C, (with rare cases up to 510 °C), or in the coercivity range 25–60 mT (rarely 80 mT), respectively (Fig. 9C–K). The Curie temperature of the magnetic carrier(s) was masked by the pyrite-to-magnetite conversion above 400 °C (Fig. 9B), as the newly formed magnetite has a much higher intensity than the original carrier.

Demagnetization diagrams were divided into three quality groups. For samples in quality group 1 (40% of all samples), the Zijderveld diagrams depict a linear decay for both declination as inclination with a feasible direction in tectonic coordinates (~360/180° and ~65/−65°). The mean angular deviation (MAD) of the vectors generally is 1–10°, with an average of 5°. For most quality 2 samples (25%), the decay of magnetic directions is less linear than for group 1, but the directions are still considered representative. Some samples in this group have directions between normal and reversed polarity. In some cases, the demagnetization pattern in the Zijderveld diagram resembles a reversed polarity with the exception that most inclinations yield positive values (Fig. 9F). Nevertheless, for these samples a reversed polarity was interpreted. The MAD of quality group 2 is between ~10 and ~20°. Quality 3 (20% of all samples) was assigned to specimens with very scattered directions, in which it was still possible to plot a magnetic vector through at least four data points. Most vectors are associated with relatively low magnetic intensities. For 15% of all demagnetized samples no vector could be plotted above 260 °C or 25 mT, and were excluded from the dataset.

Magnetic intensities in the sections GR and S1 are a factor 15 higher than in the rest of the samples (Suppl. Mat. B). In general, their samples also have the most stable magnetic vectors up to the highest temperatures and coercivities for both AF as TH. Most belong to the high quality group, and some reach 500 °C, indicating the absence of a dominant pyrite and greigite fraction.

The mean statistical test results of the reversed (R) and normal (N) groups on reliable samples (Qualities 1–2) for different sections are used to check the origin of the signals before they are used for magnetostratigraphy (Fig. 10). All reversed samples together yield a positive fold test, suggesting that the interpreted signal is primary. When we add the inverted normal polarity data of sub-sections S2 and S3, it remains positive. However, when we add the normal polarity data of S4 as well (polarity interval “Na” in Fig. 11), the fold test becomes negative. This signals that the normal directions of S4 differ slightly from the rest. The mean value of these directions is dissimilar from the present-day field in the study area (Fig. 10A), and in some specimens a low temperature component can be distinguished during thermal demagnetization (e.g., sample NR119, Fig. 9D), suggesting that most higher temperature components of S4 do not reflect a present-day overprint.

A comparison of the decay behavior during thermal demagnetization of the normal specimens in section 4 (Fig. 9J) and the other sections (Fig. 9K) demonstrates that the high temperature components of S4 account for a much lower percentage of the total NRM than in the other sections. The lower temperature directions thus make up for a

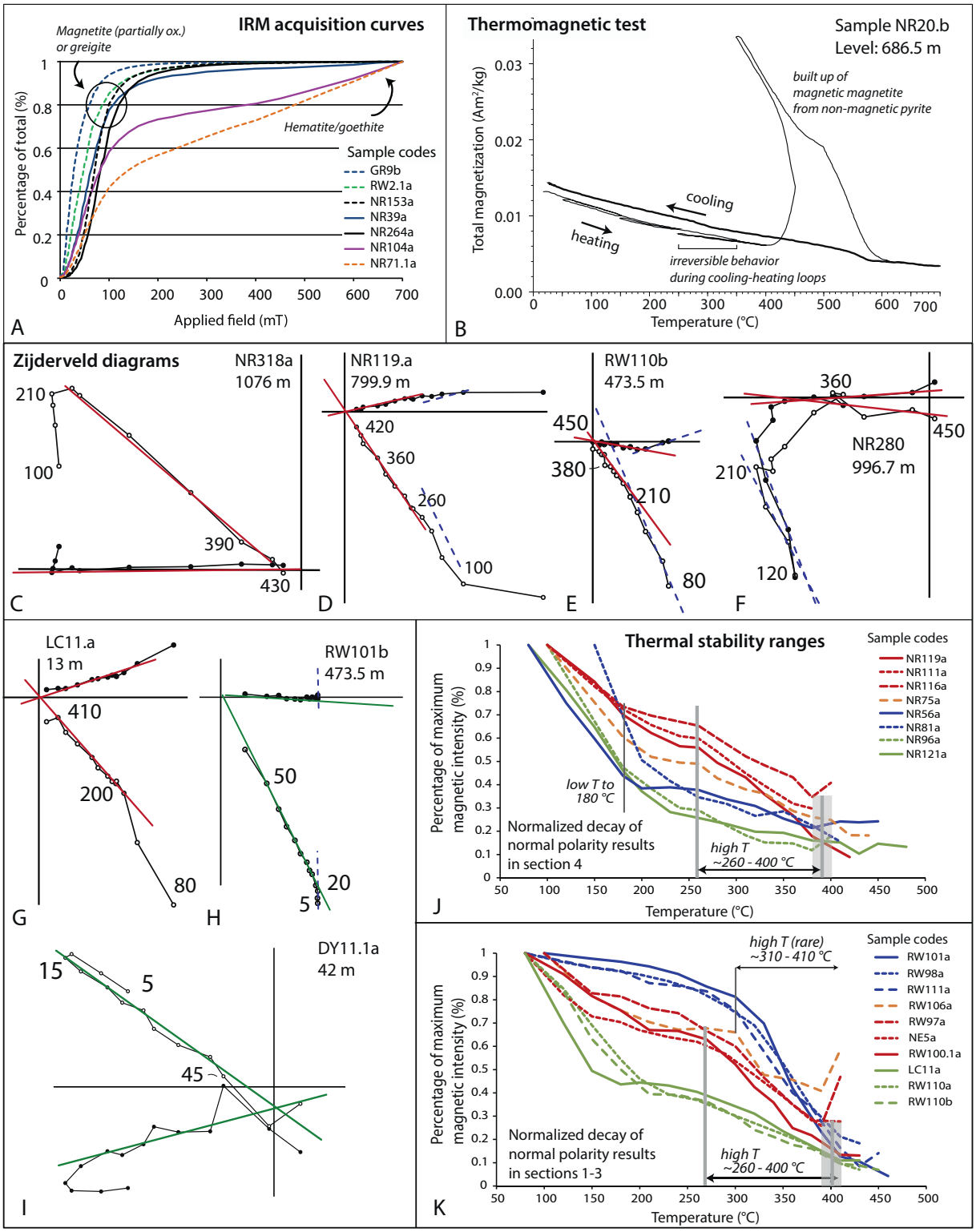


**Fig. 9.** Paleomagnetic results. Rockmagnetic and paleomagnetic data. (A) Characteristic distribution of sample behavior during Isothermal Remanent Magnetization experiments. ox. = oxidized. (B) Representative thermomagnetic diagram. (C–I) Zijderveld diagrams of thermal (C–G) and alternating field (H,I) demagnetized samples. Red (green) lines represent the high temperature/field components, dashed blue lines are the low temperature/field components. Open (closed) circles are inclination (declination) steps. Accompanying values are temperature or field steps in °C or mT. (J,K) Normalized thermal decay patterns for representative normal samples of section 4 (J) and other sections (K). Typical ranges for high/low temperature components are accentuated and are similar for most samples. (For interpretation of the references to color in this figure legend, the reader is referred to the web version of this article.)

A

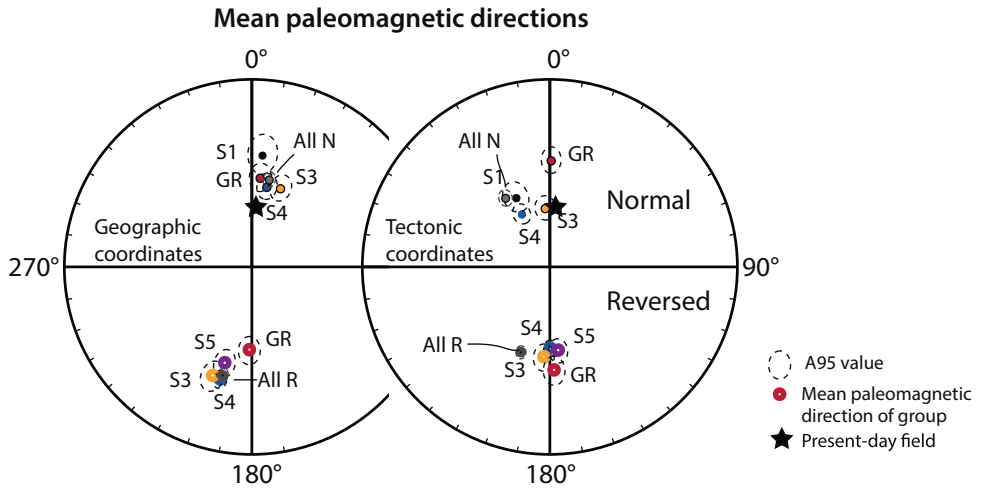


B

| Section | sub-section | n | n (45° cut) | po-larity | geographic dec | geographic inc | tectonic coordinates dec | tectonic coordinates inc | R | κ | α95 | Notes |
|---|---|---|---|---|---|---|---|---|---|---|---|---|
| MJ | S1 | 23 | 21 | N | 5.5 | 40.1 | 334.0 | 56.5 | 73.4 | 28.8 | 3.1 | |
| MJ | S2,3 | 23 | 23 | N | 20.1 | 53.4 | 355.5 | 64.5 | 35.8 | 30.1 | 4.4 | Positive fold test with All R. |
| MJ | S3 | 46 | 46 | R | 199.8 | -38.4 | 183.8 | -50.3 | 43.4 | 17.6 | 5.2 | |
| MJ | S4 | 41 | 37 | N | 10.7 | 54.5 | 332.0 | 64.1 | 22.5 | 43.4 | 4.6 | GC different from present-day field. |
| MJ | S4 | 77 | 76 | R | 195.7 | -37.9 | 179.8 | -54.4 | 20.3 | 28.2 | 6.1 | |
| MJ | S5 | 29 | 28 | R | 195.8 | -45.9 | 174.3 | -53.2 | 11.9 | 75.8 | 5.0 | |
| GR | - | 12 | 12 | R | 181.7 | -53.6 | 177.6 | -44.3 | 19.6 | 46.1 | 4.9 | |
| GR | - | 20 | 20 | N | 5.4 | 50.8 | 0.7 | 42.9 | 27.4 | 42.2 | 4.2 | |
| MJ + GR | All | 107 | 107 | N | 10.3 | 50.6 | 346.6 | 59.5 | 101.3 | 18.5 | 3.3 | Negative fold test. Not antipodal to All R. |
| MJ + GR | All | 166 | 166 | R | 195.9 | -40.5 | 180.5 | -52.1 | 157.7 | 19.9 | 2.5 | Positive fold test. |

**Fig. 10.** Paleomagnetic statistics. (A) Equal area projections of the mean ChRMs for the reliable samples of Greben (GR) and Modrinje-Janjići (MJ) section (sub-sections S1–5). (B) The table summarizes the main statistical results for the sites depicted in the equal area plots. See the main text for an explanation of the statistical implications. R = reversed, N = normal, Dec/Inc = mean declination/inclination, n = number of data in selected group, R = resultant vector length, κ = dispersion of directions, α95 = Fisher cone of confidence.

large part of the total magnetization in S4. In other words, it is more difficult to completely separate the lower temperature (often a post-sedimentary overprint) from the high temperature components when plotting the magnetic vectors in the Zijderveld diagrams. Although some measured values may deviate slightly from the original ChRM, we interpret the normal signals in section 4 (Na) to reflect the polarity of the ChRM as well (Fig. 11).

### 5.4. Magnetostratigraphic correlation to the timescale

The magnetostratigraphy of the Sarajevo-Zenica Basin is based on the results from quality groups 1 and 2 (Fig. 11). The ChRMs plotted against stratigraphic level reveal a clear magnetostratigraphic pattern above ~300 m (Fig. 12; Suppl. Mat. B). One evident phenomenon is the large amount of reversed directions in the middle-upper part of the section (Ra, Rb, Rc). The largest normal polarity intervals are present in the intervals 460–510 m (Nb) and 690–810 m (Na). Close to the reversals, at the base and top of Na, many samples with mixed polarities are present (Fig. 11), possibly reflecting a partial diagenetic overprint in the top layer of the sediment by the subsequent chron. The polarity zones in the intervals 615–625 and 1000–1020 m are marked gray because of questionable normal polarity samples in combination with samples with contradicting polarities. In general, the lowermost part of S4 yields many lower quality data points which could be related to the generally weaker magnetic intensities in this part of the section (Fig. 11).

The biostratigraphic constraints by the *Deinotherium* mammal fossil (main coal layer) and clivunnelid mollusks (up to base S4) imply a lower Miocene age for the basal part of the sampled succession, at least up to the base of S4.

The most dominant feature of the Sarajevo-Zenica polarity pattern is the large (~400 m) thick reversed polarity zone (Ra) in the uppermost part of the profile, which we thus correlate to the longest reversed chron of the GPTS; C5Br (Fig. 12). The top of Na is tied to the top of Chron C5Cn.1n, and the base of Nb to the base of C5Cn.3n, so that the reversed interval (Rc) and the unexposed part below can be linked to chron C5Cr. In this configuration the maximum age for the base of S2-b is 17.2 Ma and the shift from dominantly fine grained (S4–S5) to coarse grained sedimentation has an age around 15 Ma (Fig. 12). Naturally, deposition in the lake basin lasted longer than 15 Ma because at least 1 km of deltaic to alluvial sediments are resting on top. The onset of the deeper lake environment (within S1) should have happened slightly earlier than 17.2 Ma.

Finally, we infer that the dominantly normal polarities found in S1 and the Greben mine, and dominantly reversed polarities in the Vrtlište mine, should fall in the range 17.2–18.0 Ma (C5Dn – C5En.1r) (Fig. 12, Suppl. Mat. B). The polarity pattern in the Greben mine, a short reversed interval between two normal intervals, does not fit to the GPTS between 18 and 17 Ma, suggesting that part of the Greben section is remagnetized, or the correlation of Greben to Modrinje-Janjići is not accurate.

The available data show that our preferred magnetostratigraphic correlation described above is not unambiguous, but it is the one that correlates best with the biostratigraphy and expected trend in

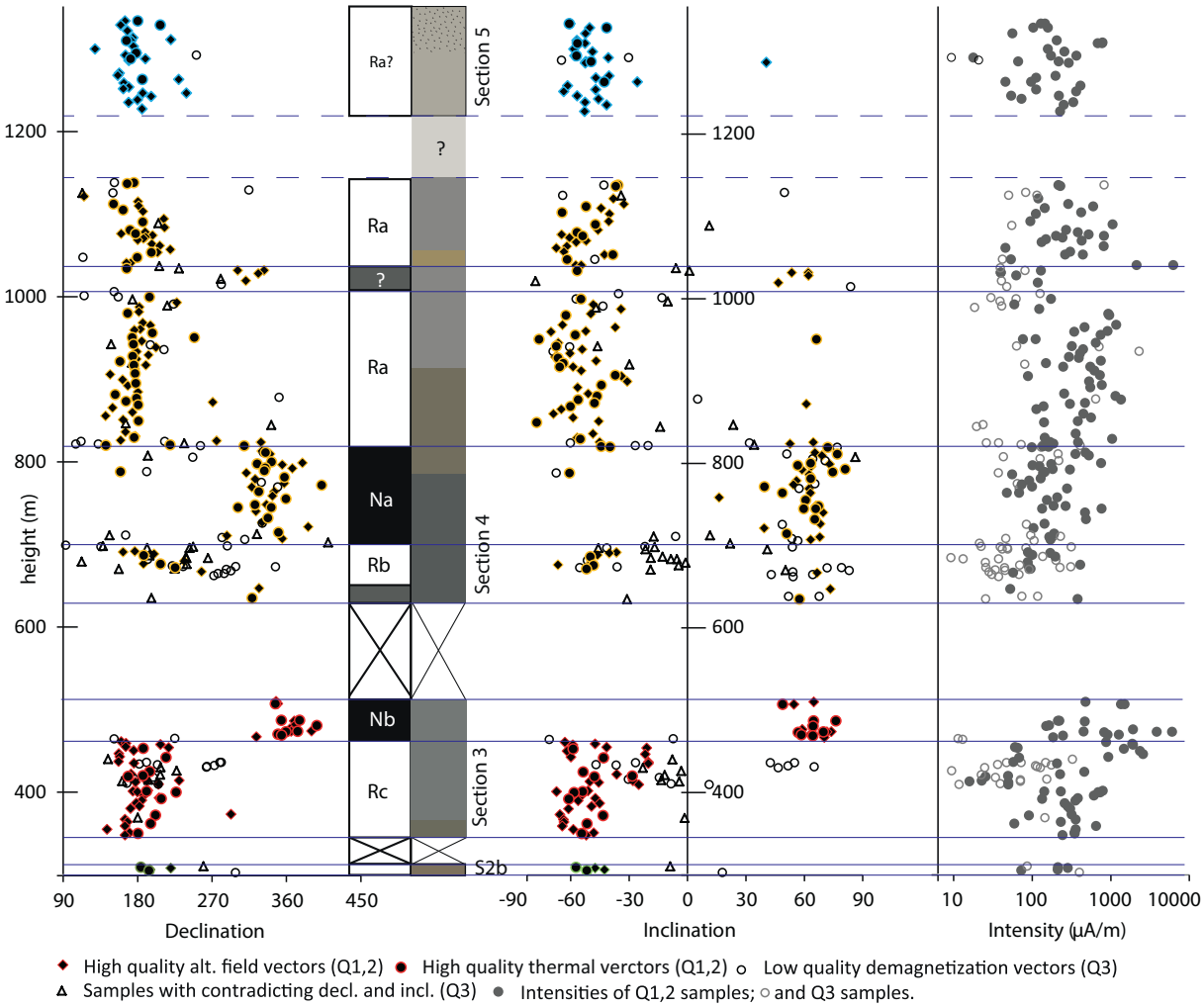


**Fig. 11.** Magnetostratigraphic results and polarity column - for sections 2-b to 5 of the Modrinje-Janjići composite section. Different colors are used for each section. Reversed/normal polarity intervals are shown in white/black and named (Ra, Na etc.). Gray zones depict uncertain polarity intervals. Magnetostratigraphic results of Vrtlište, Greben and sections 1 and 2-a are placed in supplementary material C, because they are of minor importance for the magnetostratigraphic correlation (Fig. 12).

sedimentation (i.e. no sudden changes in sedimentation rates). One other possible correlation would be to correlate the full sequence to the middle Miocene chrons C5ADn to C5Ar.1r (~14.6–12.5 Ma). However, this drastically younger correlation does not fit with the presence of primitive dreissenid bivalves in the basal marls (~S2; Muftić, 1965) and the base of S4 (Table 1), which were so far only found in lower Miocene DLS sediments (de Leeuw et al., 2011b). Other alternative correlations are also possible when significant stratigraphic gaps are implied, although such gaps were not observed in our data.

## 6. Sarajevo-Zenica Basin stratigraphy in the context of the Dinaride Lakes System

### 6.1. The "Oligo-Miocene" basin phase

The main coal seam (uppermost VR section) is the lowermost layer in the stratigraphy found to wedge towards the south-western basin margin (Milojević, 1964). Given the available correlation with normal faulting (see also Andrić et al., 2017), the deposition of this seam was syn-kinematic, marking the onset of the normal faulting along the Busovača fault system. The *Deinotherium* fossil (Milojković, 1929) in the coal seam shows that this evolutionary basin phase started the earliest ~18.4 Ma.

These observations show that the underlying Oligo-Miocene sediments are at least 18.5 Ma old, which is in agreement with our magnetostratigraphic correlation (sediments below S2b > 17.2 Ma, Fig. 12). Our detailed observations have identified local unconformities related to reverse faults activation in this sequence, but a major regional correlative stratigraphic hiatus in the "Oligo-Miocene" sequence (Milojević, 1964) was not confirmed. Therefore, we interpret that the sediments in the Vrtlište mine below the main coal layer, and the majority of the Bijele Vode section were deposited during the early Miocene. This is supported by the fact that the clivunellid gastropods, which are restricted to the lower Miocene, were reported in the unit correlating to the BV section, and that no typical Oligocene ostracods were encountered in the entire succession (Muftić, 1965).

It is possible that the basal Koscani coal seam correlates to the coals in Lake Banovići and Ugljevik (de Bruijn et al., 2013; de Leeuw et al., 2011a; Glišić et al., 1976; Wessels et al., 2008). In Banovići, the coal and overlying lacustrine carbonates were magnetostratigraphically dated to be ~24 Ma (de Leeuw et al., 2011a), concurring with the Late Oligocene Climatic Optimum (Fig. 12) (Mosbrugger et al., 2005; Zachos et al., 2001). This climatic phase might have also supported the formation of the basal Koscani coal and limestones. At the same time, syn-kinematic deposition and formation of local unconformities in the Bijele Vode area, shows that deposition of the oldest part of the Oligo-Miocene succession occurred during a NE-SW contraction event. This event was associated with pulses of thrusting and loading that created the

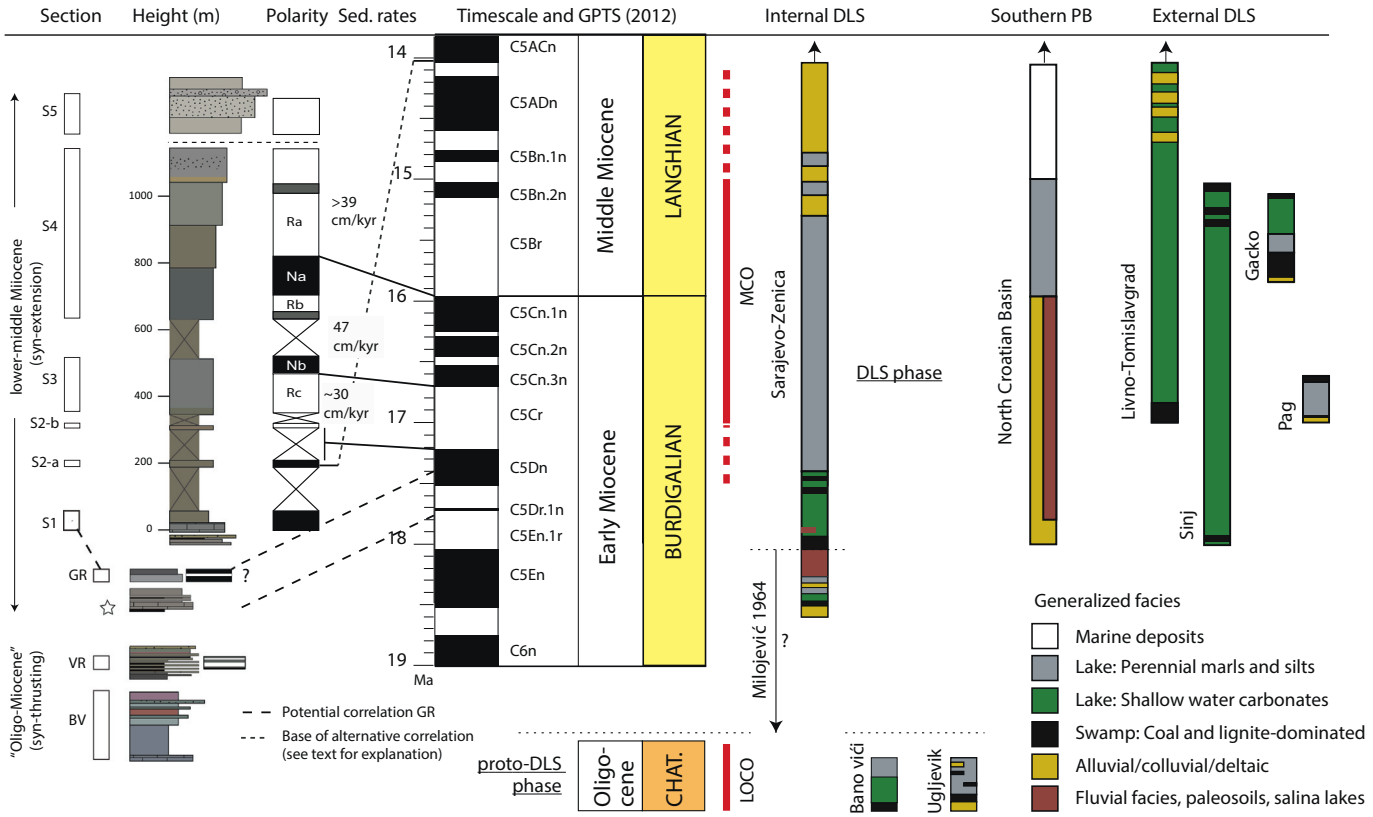


**Fig. 12.** Magnetostratigraphic correlation - of the lower-middle Miocene lacustrine phase of the Sarajevo-Zenica Basin and the estimated position of the underlying succession (left), together with an overview of the lakes of the lower-middle Miocene lacustrine DLS phase and older Dinaride (see Fig. 1B for their locations). Note that the older DLS basin infills are not dated, except for Banovići and Ugljevik (right). Timescale and global polarity time scale (GPTS) after Hilgen et al. (2012). MCO = Miocene Climatic Optimum. LOCO = Late Oligocene Climatic Optimum.

foredeep accommodation space and formed an active source area shedding significant clastic sediments into the basin (see also) (Andrić et al., 2017).

From the basal Koscani coal seam up to the main coal seam, the paleoenvironments changed from palustrine to shallow lacustrine settings, and then to dominantly distal fluvial facies with at least one prominent palustrine phase (coal and packstones). These alternations suggest that the lake base level changes were controlled by the interplay of climate-induced regional retrogradation and the episodic thrusting, which increased the local foredeep accommodation space, while the source area diminished the influx of clastic sediments. Such an interplay between climate an tectonics is a common phenomenon observed in other worldwide basins (e.g., Alonso-Zarza and Calvo, 2000; Cohen, 2003b).

Similar tectono-sedimentary relationships in the Internal Dinarides are poorly constrained, but in the coastal regions of the External Dinarides foreland basin settings are known from Oligocene times. In the distal parts, syn-kinematic sedimentation (Promina Beds) took place in piggy-back and local foredeep basins (Babić and Županić, 1983; Babić and Županič, 1988; Ivanović et al., 1973; Županić and Babić, 2011). The inferred early Miocene age for the majority of the Oligo-Miocene succession implies that syn-contractional deposition in the Sarajevo-Zenica Basin has lasted longer than inferred elsewhere in the Dinarides, where this tectonic event if generally thought to be Eocene – early Oligocene in age.

At higher resolution, the fluctuations in the Oligo-Miocene paleoenvironment of the Sarajevo-Zenica Basin might have been affected by cyclic fluctuations in humidity, for example by creating the distinctive red paleosoils (BV2) during drier (semi-arid) periods, or coal-limestone alternations (VR). However, these signals cannot be quantified in this part of the sedimentary record in the absence of further higher resolution age constraints.

### 6.2. *The lower-middle Miocene lake basin: climate vs tectonics*

The second evolutionary phase in the Sarajevo-Zenica Basin started the earliest at ~18.4 Ma, as demonstrated by the onset of syn-kinematic deposition that created the wedging of the main coal layer during the normal faulting induced by the Busovača Fault system. According to our magnetostratigraphic correlation, a deepening of the Sarajevo-Zenica Lake happened at least at 17.2 Ma, and the lacustrine environment persisted at least up to 15 Ma.

The timing of the long-lived lake phase in the Sarajevo-Zenica Basin is coeval to many of its sister lakes in the External Dinarides, including the Livno-Tomislavgrad, Pag and Sinj Basins (de Leeuw et al., 2010, 2011b) (Fig. 12). The long-lived lake phases of all DLS basins are coeval with the transition to and peak of the MCO (17–15 Ma; Holbourn et al., 2005), implying that the paleoenvironments were affected by the MCO, and the transitional period towards the optimum. A subtropical climate with a strong seasonality in precipitation existed in SE Europe in the Burdigalian, marking the onset of the MCO (Jiménez-Moreno et al., 2009; Pavelić et al., 2016). In the Pag Basin, an increase in xerophilous pollen suggests a gradual warming and drying of the climate (~17–16 Ma) (Jiménez-Moreno et al., 2009). The drier and warmer periods were most likely amplified by eccentricity cycles, which were recognized in alternating limestone and lignite intervals, in distal parts of DLS basins, for example in Pag and Gacko (Jiménez-Moreno et al., 2009; Mandic et al., 2011). In the Požega basin of the North Croatian lakes, wet periods with braided alluvial fan deposition alternated with arid periods marked by loess-like deposition and cycles in a salina-type lake (~18–16 Ma) (Pavelić et al., 2016; Pavelić and Kovačić, 1999; Šćavničar et al., 1983).

In the Sarajevo-Zenica Basin, the first sign of a warmer climate was found at the base of the extensional basin phase, where the main coal seam yielded plant remains of moderate-warm deciduous forests (Pantić et al., 1966). The palustrine phase transitioned into the limestone-dominated shallow lake phase (S1), in which several small-scale (dm-scale) alternations of limestones and coaly silts most probably reflect short-term fluctuations in base level or sediment influx (Fig. 5C). The alternations might have formed in response to climate-induced base level changes, but could not be quantified in this study (Fig. 8B).

No clear cyclic behavior was observed in the overlying perennial to delta succession (S2–S5). The magnetostratigraphic framework indicated sediment accumulation rates of ~30 cm/kyr in the marl-dominated base (S2b-3), ~47 cm/kyr in the middle (S4a) and higher than 39 cm/kyr in the sand-rich top (S4b-c) of the Sarajevo-Zenica lacustrine phase (Fig. 12). The average sedimentation rate for the whole studied profile (300–1140 m) is > 40 cm/kyr. The increasing rates concur with the gradual increase in siliciclastic input visible since ~17 Ma, which is related to the footwall uplift along the Busovača Fault zone at the SW basin margin (Andrić et al., 2017).

In the tectono-sedimentary basin model for the Sarajevo-Zenica Basin by Andrić et al. (2017), slip along a low-angle listric fault causes rapid basin deepening that is then followed by enhanced footwall uplift (steeper footwall gradient) creating a progradation. Abrupt shifts towards finer sedimentation, such as on top of S5, are directly related to back-stepping of such a syn-sedimentary fault (Andrić et al., 2017; Miall, 1978). Numerical modeling suggests that after an asymmetric basin is perturbed by fault slip, it takes ~1 Myr for the system to reach a new steady state (Armitage et al., 2011). In light of this, it is logical that no clear Milankovitch scale climate cycles were encountered in the majority of the studied sections, because these tectonic signals had a much higher effect in terms of offsets and associated rates of sedimentation. Most importantly, it suggests that the majority of the lacustrine infill of the Sarajevo-Zenica Basin, at least after 15 Ma, was tectonically controlled.

In most paleolakes of the External Dinarides, mean sedimentation rates were lower than in the Sarajevo-Zenica Basin, for example in the Sinj (10–20 cm/kyr), Gacko (10–30 cm/kyr) and Pag (> 22 cm/kyr) basins (de Leeuw et al., 2010; Jiménez-Moreno et al., 2009; Mandic et al., 2009, 2011), implying that these basins were generated in a setting with lower subsidence compared to the Sarajevo-Zenica Basin. Lake Sinj was dominated by limestones and marls in the distal areas, but conglomerates found nearby the former basin margin suggest that a steep basin slope existed, which could reflect an uplifted footwall. In the Livno-Tomislavgrad Basin forms, sedimentation rates increased from 37 to ~55 cm/kyr (de Leeuw et al., 2011b), which might suggest subsidence rates comparable to the Sarajevo-Zenica Basin.

Similar as in the DLS, the majority of lacustrine deposition in the North Croatian lakes of the southern Pannonian basin (NCB; Fig. 1B) took place in the Burdigalian (Kovačić, 2016; Mandic et al., 2012; Pavelić and Kovačić, 2018). Lacustrine deposition was subsequently terminated by a marine flooding event (~15–14 Ma) (Ćorić et al., 2009; Pavelić and Kovačić, 2018). Lake Popovac, situated to the east of the Dinarides, formed in the middle Miocene (~15–14 Ma) (Krstić et al., 2003; Sant et al., 2018). Thus, most of these lakes existed during the (final phase of the) MCO and their basin formation also directly correlates to the large-scale Pannonian back-arc rifting phase (Pavelić, 2001).

Despite some fining upwards pulses, the early-middle Miocene Sarajevo-Zenica Lake disappeared around ~15–14 Ma, marking the cessation of the main extension phase. Lake deposition in the Sinj and Gacko Basins terminated around 15 Ma as well (de Leeuw et al., 2010; Mandic et al., 2009, 2011). In the Sinj Basin, the final stage of basin filling comprises two shallowing upward cycles with limestones to coal seams. In the Livno-Tomislavgrad basin, a shift to more siliciclastic/land-derived sedimentation started ~15 Ma. Its limestones graded into laminated limy sediments and coarser influxes like calcarenites, limestone pebbles, slumps, debrites and breccias occurred at least until 13 Ma (de Leeuw et al., 2011b).

The overall shallowing and disappearance of the middle Miocene lakes of the DLS overlaps with the decline of the MCO commencing after ~15–14 Ma (Böhme, 2003; Holbourn et al., 2014), when drier conditions were gradually installed in the Pannonian and Balkan regions (Utescher et al., 2007) (Fig. 12).

All these observations and correlations show that the onset and cessure of the normal faulting and MCO were coeval in the Sarajevo-Zenica Basin and possibly also elsewhere in the Dinarides. Whether there is a genetic link between the two processes at the scale of the entire orogen is rather speculative and outside the scope of our study. But one could imagine a temporary switch from contraction to extension controlled by a gravitational disequilibrium created by a substantial increase in the amount of orogenic erosion triggered by humid conditions during the MCO.

## 7. Conclusions

Our new bio-magnetostratigraphic and sedimentary data of the Sarajevo-Zenica Basin allow for a quantitative comparison of its paleoenvironmental evolution to the evolution of other Dinaride Lake System basins. The Sarajevo-Zenica Basin has the additional advantage that the paleoenvironmental evolution can be compared to the coeval tectonics, leading to valuable insights into the effects of climatic and geodynamic events on the paleogeographic evolution of the Dinaride Lake System.

The Oligo-Miocene series were deposited in shallow lacustrine, palustrine, swamp and flood-plain dominated river environments that reflect base level fluctuations, which could be controlled by phases of tectonic loading during the final phase of nappe stacking in the Internal Dinarides. The succession is older than ~18.5–17.5 Ma. Based on lower Miocene clivunnelid mollusks and Miocene ostracods, the studied interval is tentatively attributed to the early Miocene, which contrasts with the previous interpretations of a largely Oligocene thrusting event.

The overlying perennial lake sediments of the extensional phase were magnetostratigraphically correlated to chrons C5Cr to C5Br (17.2 to ~15.0 Ma), which is in agreement with the occurrence of lower Miocene clivunnelid gastropods in the basal marls of the succession. Deposition overlaps with the main period of lacustrine deposition in the External DLS lakes, and largely with the onset and peak of the Miocene Climatic Optimum, suggesting that like in the other DLS and other lakes in the southern Pannonian Basin, the humidity during the MCO must have helped to sustain the lacustrine environment.

The clastic deposits of the first thrusting basin phase were exclusively derived from the northern Ophiolite Complex and Bosnian Flysch sources, whereas during the second normal faulting phase, at least since 17.2 Ma, most material derived from the southern Bosnian Schist Mountains and its overlying sedimentary cover.

The central part of the Sarajevo-Zenica Basin experienced a gradually increasing input of siliciclastic material since ~17 Ma until deltaic to alluvial settings prevailed in the middle Miocene (after ~15 Ma in the study area). This is accompanied by increasing sedimentation rates from ~30 cm/kyr to > 40–50 cm/kyr. Activity in the extensional Busovača low-angle normal fault zone likely was the major control on the paleoenvironmental and sedimentological evolution during the lower-middle Miocene lake phase of the basin.

The rapid sedimentation recorded by the Sarajevo-Zenica Basin after 15 Ma is coeval with the onset of drier conditions that resulted from the cessation of the MCO, and also marks the end of the extensional phase. Around the same time, a shift to coarser sedimentation was noted in the DLS basins in the External Dinarides, when Lake Sinj and Gacko terminated. This suggests that these basins were affected by the same processes as the Sarajevo-Zenica Basin. Our observations demonstrate a conspicuous overlap between the onset of a warmer and more humid climate during the Miocene Climatic Optimum and the

large-scale extension phase in the Sarajevo-Zenica Basin. Whether this is a generalized correlation at the scale of the Dinarides triggered by a yet unknown tectonic-climate interaction is likely the subject of further studies.

## Acknowledgments

Special thanks go to the helpful staff of the Bosnian Geological Society, in particular to Alojz Filipović and Ćazim Šarić for their warm support during the entire field campaign. Besides this, we are indebted to Jolien Ooms, Seán Morley and Haris Hodžić (Brown Coal Mine Kakanj) for their field assistance, and Roel van Elsas and Leonard Blik for lab support. Klaudia Kuiper is thanked for the cooperation in the $^{40}Ar/^{39}Ar$ laboratory. We are also grateful for advice by Cor Langereis concerning paleomagnetic statistics, and by Mark Dekkers on rock magnetic details. This research was financially supported through the Netherlands Geosciences Foundation (ALW) with funding from the Netherlands Organization for Scientific Research (NWO) by VICI grant 865.10.011 of WK. NA was financed by the Netherlands Research Centre for Integrated Solid Earth Science (ISES). In addition, the Ministry of Education and Science of the Republic of Serbia financially supported NA and LjR via project number OI176019 and OI176015, respectively. We are grateful for the constructive feedback received from Miguel Garces and an anonymous reviewer.

## Appendix A. Supplementary data

Supplementary data associated with this article can be found in the online version, at doi:https://doi.org/10.1016/j.palaeo.2018.06.009. These data include the Google map of the most important areas described in this article.

## References

Albrecht, C., Wilke, T., 2008. Ancient Lake Ohrid: biodiversity and evolution. Hydrobiologia 615, 103–140. http://dx.doi.org/10.1007/s10750-008-9558-y.
Alonso-Zarza, A.M., Calvo, J.P., 2000. Palustrine sedimentation in an episodically subsiding basin: the Miocene of the northern Teruel Graben (Spain). Palaeogeogr. Palaeoclimatol. Palaeoecol. 160, 1–21. http://dx.doi.org/10.1016/S0031-0182(00)00041-9.
Alonso-Zarza, A.M., Wright, V.P., 2010. Palustrine carbonates. In: Developments in Sedimentology, pp. 103–131. http://dx.doi.org/10.1016/S0070-4571(09)06102-0.
Andrić, N., Sant, K., Matenco, L., Mandic, O., Tomljenović, B., Pavelić, D., Hrvatović, H., Demir, V., Ooms, J., 2017. The link between tectonics and sedimentation in asymmetric extensional basins: inferences from the study of the Sarajevo-Zenica Basin. Mar. Pet. Geol. 83, 305–332. http://dx.doi.org/10.1016/j.marpetgeo.2017.02.024.
Armitage, J.J., Duller, R.A., Whittaker, A.C., Allen, P.A., 2011. Transformation of tectonic and climatic signals from source to sedimentary archive. Nat. Geosci. 4, 231–235. http://dx.doi.org/10.1038/ngeo1087.
Atabey, E., Atabey, N., Kara, H., 1998. Sedimentology of caliche (calcrete) occurrences of the Kirşehir region. Miner. Res. Explor. Bull. 120, 69–80.
Aubouin, J., Blanchet, R., Cadet, J.-P., Celet, P., Charvet, J., Chorowicz, J., Cousin, M., Rampnoux, J.-P., 1970. Essai sur la géologie des Dinarides. Bull. Soc. Géol. Fr. 12, 1060–1095.
van Baak, C.G.C., Vasiliev, I., Palcu, D.V., Dekkers, M.J., Krijgsman, W., 2016. A Greigite-based magnetostratigraphic time frame for the Late Miocene to recent DSDP leg 42B cores from the Black Sea. Front. Earth Sci. 4, 1–18. http://dx.doi.org/10.3389/feart.2016.00060.
Babić, L., Županić, J., 1983. Paleogene clastic formations in northern Dalmatia. In: Babic, L., Jelaska, V. (Eds.), Contributions to Sedimentology of Some Carbonate and Clastic Units of the Coastal Dinarides. Excursion Guidebook: International Association of Sedimentologists 4th Regional Meeting. Association of Sedimentologists, Split, pp. 37–61.
Babić, L., Županič, J., 1988. Coarse-grained alluvium in the Paleogene of northern Dalmatia (Croatia, Yugoslavia). Rad JAZU 441, 139–164.
Bechtel, A., Markic, M., Sachsenhofer, R.F., Jelen, B., Gratzer, R., Lücke, A., Püttmann, W., 2004. Paleoenvironment of the upper Oligocene Trbovlje coal seam (Slovenia). Int. J. Coal Geol. 57, 23–48.
Böhme, M., 2003. The Miocene climatic optimum: evidence from ectothermic vertebrates of Central Europe. Palaeogeogr. Palaeoclimatol. Palaeoecol. 195, 389–401. http://dx.doi.org/10.1016/S0031-0182(03)00367-5.
Böhme, M., Aiglstorfer, M., Uhl, D., Kullmer, O., 2012. The antiquity of the Rhine River: stratigraphic coverage of the Dinotheriensande (Eppelsheim Formation) of the Mainz basin (Germany). PLoS One 7. http://dx.doi.org/10.1371/journal.pone.0036817.
Bown, T.M., Kraus, M.J., 1987. Integration of channel and floodplain suites, I. Developmental sequence and lateral relations of alluvial paleosols. J. Sediment. Petrol. 57, 587–601.
Brady, G.S., Norman, A.M., 1889. A monograph of the marine and freshwater Ostracoda of the north Atlantic and of Northwestern Europe. Section I. Podocopa. Sci. Trans. R. Dublin Soc. Ser. 2 (4), 63–270.
de Bruijn, H., Marković, Z., Wessels, W., 2013. Late Oligocene rodents from Banovići (Bosnia and Herzegovina). Palaeodiversity 6, 63–105.
de Bruijn, H., Marković, Z., Wessels, W., Milivojević, M., van de Weerd, A.A., 2017. Rodent faunas from the Paleogene of south-east Serbia. Palaeobiodivers. Palaeoenviron. http://dx.doi.org/10.1007/s12549-017-0305-0. (in press).
Casale, G.M., 2012. Core Complex Exhumation in Peri-Adriatic Extension, and Kinematics of Neogene Slip along the Saddle Mountains Thrust. University of Washington.
Chou, C.-L., 2012. Sulfur in coals: a review of geochemistry and origins. Int. J. Coal Geol. 100, 1–13.
Cohen, A.S., 2003a. Paleolimnology: The History and Evolution of Lake System. Oxford University Press, Oxford.
Cohen, A.S., 2003b. The physical environment of lakes. In: Cohen, A.S. (Ed.), Paleolimnology: The History and Evolution of Lake System. Oxford University Press, Oxford, pp. 56–68.
Cohen, A.S., 2003c. Geochemical archives in lake deposits. In: Cohen, A.S. (Ed.), Paleolimnology: The History and Evolution of Lake System. Oxford University Press, Oxford, pp. 241–272.
Cohen, A.S., 2003d. Sedimentological archives in lake deposits. In: Cohen, A.S. (Ed.), Paleolimnology: The History and Evolution of Lake System. Oxford University Press, Oxford, pp. 162–207.
Ćorić, S., Pavelić, D., Rögl, F., Mandic, O., Vrabac, S., 2009. Revised Middle Miocene datum for initial marine flooding of North Croatian Basins (Pannonian Basin System, Central Paratethys). Geol. Croat. 62, 31–43.
Dankers, P.H.M., Zijderveld, J.D.A., 1981. Alternating field demagnetization of rocks, and the problem of gyromagnetic remanence. Earth Planet. Sci. Lett. 53, 89–92.
Dimitrijević, M.D., 1997. Geology of Yugoslavia, Geol. Inst. Gemini Spec. Publ. Barex, Belgrade.
Dragičević, I., Hrvatović, H., Vranjković, A., Mandic, O., Šegvić, B., Halamić, J., Pavelić, D., 2010. Excursion A1 - dinarides: evolution and recent geotectonic relationships (Bosnia and Herzegovina, Croatia). In: 4th Croatian Geological Congress Guide Book. Croatian Geological Society, Šibenik, pp. 27–88.
Džindo, M., 2013. Elaborat o klasifikaciji, kategorizaciji i proračunu rezervi oraškog ugljenog sloja u ležištu "'Vrtlište'" Rudnika mrkog uglja "Kakanj" (Elaborate on classification, categorization and calculation of Oraški coal layer reserves in the deposit 'Vrtlište'). Tuzla.
Erak, D., Matenco, L., Toljić, M., Stojadinović, U., Andriessen, P.A.M., Willingshofer, E., Ducea, M.N., 2017. From nappe stacking to extensional detachments at the contact between the Carpathians and Dinarides – the Jastrebac Mountains of Central Serbia. Tectonophysics 710–711, 162–183. http://dx.doi.org/10.1016/j.tecto.2016.12.022.
Fisher, R., 1953. Dispersion on a sphere. Proc. R. Soc. A Math. Phys. Eng. Sci. 217, 295–305. http://dx.doi.org/10.1098/rspa.1953.0064.
Fodor, L., Csontos, L., Bada, G., Gyorfi, I., Benkovics, L., 1999. Tertiary tectonic evolution of the Pannonian Basin system and neighbouring orogens: a new synthesis of palaeostress data. Geol. Soc. Lond. Spec. Publ. 156, 295–334. http://dx.doi.org/10.1144/gsl.sp.1999.156.01.15.
Freytet, P., Verrecchia, E.P., 2002. Lacustrine and palustrine carbonate petrography: an overview. J. Paleolimnol. 27, 221–237. http://dx.doi.org/10.1023/A:1014263722766.
Glišić, R., Dangić, A., Milojević, R., Milojević, R., 1976. Ugljenonosni basen Banovići (Coal basin Banovici). In: Mineralne Sirovina Bosne i Hercegovine. Knjiga I. Ležišta. Uglja. Geoinžinjering, Sarajevo, pp. 58–73.
Gross, M., 2008. A limnic ostracod fauna from the surroundings of the Central Paratethys (Late Middle Miocene/Early Late Miocene; Styrian Basin; Austria). Palaeogeogr. Palaeoclimatol. Palaeoecol. 264, 263–276. http://dx.doi.org/10.1016/j.palaeo.2007.03.054.
Hajek-Tadesse, V., Belak, M., Sremac, J., Vrsaljko, D., Wacha, L., 2009. Early Miocene ostracods from the Sadovi section (Mt Požeška gora, Croatia). Geol. Carpath. 60, 251–262. http://dx.doi.org/10.2478/v10096-009-0017-0.
Harzhauser, M., Mandic, O., 2008. Neogene lake systems of Central and South-Eastern Europe: faunal diversity, gradients and interrelations. Palaeogeogr. Palaeoclimatol. Palaeoecol. 260, 417–434. http://dx.doi.org/10.1016/j.palaeo.2007.12.013.
Heslop, D., Dekkers, M.J., Kruiver, P.P., van Oorschot, I.H.M., 2002. Analysis of isothermal remanent magnetization acquisition curves using the expectation-maximization algorithm. Geophys. J. Int. 148, 58–64. http://dx.doi.org/10.1046/j.0956-540x.2001.01558.x.
Hilgen, F.J., Lourens, L.J., Van Dam, J.A., 2012. The Neogene Period. In: The Geologic Time Scale 2012. Volume 2. pp. 923–978.
Holbourn, A., Kuhnt, W., Schulz, M., Erlenkeuser, H., 2005. Impacts of orbital forcing and atmospheric carbon dioxide on Miocene ice-sheet expansion. Nature 438, 483–487. http://dx.doi.org/10.1038/nature04123.
Holbourn, A., Kuhnt, W., Lyle, M., Schneider, L., Romero, O., Andersen, N., 2014. Middle Miocene climate cooling linked to intensification of eastern equatorial Pacific upwelling. Geology 42, 19–22. http://dx.doi.org/10.1130/G34890.1.
Holbourn, A., Kuhnt, W., Kochhann, K.G.D., Andersen, N., Meier, S.K.J., 2015. Global perturbation of the carbon cycle at the onset of the Miocene Climatic Optimum. Geology 43, 123–126. http://dx.doi.org/10.1130/G36317.1.
Horváth, F., Musitz, B., Balázs, A., Végh, A., Uhrin, A., Nádor, A., Koroknai, B., Pap, N., Tóth, T., Wórum, G., 2015. Evolution of the Pannonian basin and its geothermal resources. Geothermics 53, 328–352. http://dx.doi.org/10.1016/j.geothermics.2014.07.009.
Hrvatović, H., 2006. Geological Guidebook Through Bosnia and Herzegovina. Geological

Survey of Bosnia and Herzegovina, Sarajevo.
Hrvatović, H., Pamić, J., 2005. Principal thrust-nappe structures of the Dinarides. Acta Geol. Hung. 48, 133–151. http://dx.doi.org/10.1556/AGeol.48.2005.2.4.
Hüsing, S.K., Dekkers, M.J., Franke, C., Krijgsman, W., 2009. The Tortonian reference section at Monte dei Corvi (Italy): evidence for early remanence acquisition in greigite-bearing sediments. Geophys. J. Int. 179, 125–143. http://dx.doi.org/10.1111/j.1365-246X.2009.04301.x.
Ivanović, A., Sakač, K., Marković, S., Sokac, B., Susnjar, M., Nikler, L., Susnjara, A., 1973. Osnovna Geoloska Karta SFRJ 1:100.000. List Obrovac. Basic Geological Map of SFRY, Obrovac Sheet.
Jiménez-Moreno, G., Mandic, O., Harzhauser, M., Pavelić, D., Vranjković, A., 2008. Vegetation and climate dynamics during the early Middle Miocene from Lake Sinj (Dinaride Lake System, SE Croatia). Rev. Palaeobot. Palynol. 152, 270–278. http://dx.doi.org/10.1016/j.revpalbo.2008.05.005.
Jiménez-Moreno, G., de Leeuw, A., Mandic, O., Harzhauser, M., Pavelić, D., Krijgsman, W., Vranjković, A., 2009. Integrated stratigraphy of the Early Miocene lacustrine deposits of Pag Island (SW Croatia): palaeovegetation and environmental changes in the Dinaride Lake System. Palaeogeogr. Palaeoclimatol. Palaeoecol. 280, 193–206. http://dx.doi.org/10.1016/j.palaeo.2009.05.018.
Jovanović, R., Mojićević, M., Tokić, S., Rokić, L., 1971. Basic Geological Map of the SFRY, 1:100.000, Sheet Sarajevo (K-34I).
Jurišić-Polšak, Z., Krizmanić, K., Hajek-Tadesse, V., 1993. Freshwater Miocene of Krbavsko Polje in Lika (Croatia). Geol. Croat. 46, 213–228.
Kirschvink, J.L., 1980. The least-squares line and plane and the analysis of palaeomagnetic data. Geophys. J. Int. 62, 699–718. http://dx.doi.org/10.1111/j.1365-246X.1980.tb02601.x.
Kochansky-Devidé, V., Slišković, T., 1972. Revizija roda Clivunella Katzer, 1918 i Delminella n.gen. (Gastropoda). Geološki Glas. Sarajev. 16. pp. 47–70.
Kochansky-Devidé, V., Slišković, T., 1978. Miocenske kongerije Hrvatske, Bosne i Hercegovine. Palaeontol. jugoslavica. 19. pp. 1–98.
Koufos, G.D., Zouros, N., Mourouzidou, O., 2003. Prodeinotherium bavaricum (Proboscidea, Mammalia) from Lesvos island, Greece; the appearance of deinotheres in the Eastern Mediterranean. Geobios 36, 305–315. http://dx.doi.org/10.1016/S0016-6995(03)00031-7.
Marković, F., Kuiper, K., Hajek-Tadesse, V., Bakrac, K., Derek, T., 2016. Age constraint on disintegration of the initial Pannonian Basin lake system. In: Kovačić, M., Mandic, O., Mandic, O., Pavelić, D., Kovačić, M., Sant, K., Andrić, N., Hrvatović, H. (Eds.), Field Trip Guide-Book. Lake - Basin - Evolution, RCMNS Interim Colloquium 2016. Croatian Geological Society, Zagreb, pp. 19–21.
Koymans, M.R., Langereis, C.G., Pastor-Galán, D., van Hinsbergen, D.J.J., 2016. Paleomagnetism.org: an online multi-platform open source environment for paleomagnetic data analysis. Comput. Geosci. 93, 127–137. http://dx.doi.org/10.1016/j.cageo.2016.05.007.
Krstić, N., 1972. Rod Candona (Ostracoda) iz kongerijskih slojeva juznog dela Panonskog Basena. [Genus Candona (Ostracoda) from Congerian Beds of Southern Pannonian Basin]. Srpska Akademija Nauka Umetnosti, Posebna Izdanja, Beograd.
Krstić, N., Savić, L., Jovanović, G., Bodor, E., 2003. Lower Miocene lakes of the Balkan Land. Acta Geol. Hung. 46, 291–299. http://dx.doi.org/10.1556/AGeol.46.2003.3.4.
Krstić, N., Olujić, J., Đajić, S., Đorđević-Milutinović, D., Tanasković, L., 2009. Fossils from the drill hole GS-1 near Gacko, SE Dinaric Alps. Bull. Nat. Hist. Mus. 2, 35–61.
Krstić, N., Savic, L., Jovanovic, G., 2012. The Neogene lakes on the Balkan land. Geol. An. Balk. Poluostrva (73), 37–60. http://dx.doi.org/10.2298/GABP1273037K.
Kruiver, P.P., Dekkers, M.J., Heslop, D., 2001. Quantification of magnetic coercivity components by the analysis of acquisition curves of isothermal remanent magnetisation. Earth Planet. Sci. Lett. 189, 269–276. http://dx.doi.org/10.1016/S0012-821X(01)00367-3.
de Leeuw, A., 2011. Paleomagnetic and Geochronologic Constraints on the Miocene Evolution of Semi-isolated Basins in Southeastern Europe. Utrecht University.
de Leeuw, A., Mandic, O., Vranjković, A., Pavelić, D., Harzhauser, M., Krijgsman, W., Kuiper, K.F., 2010. Chronology and integrated stratigraphy of the Miocene Sinj Basin (Dinaride Lake System, Croatia). Palaeogeogr. Palaeoclimatol. Palaeoecol. 292, 155–167. http://dx.doi.org/10.1016/j.palaeo.2010.03.040.
de Leeuw, A., Mandic, O., de Bruijn, H., Marković, Z., Reumer, J., Wessels, W., Šišić, E., Krijgsman, W., 2011a. Magnetostratigraphy and small mammals of the Late Oligocene Banovići basin in NE Bosnia and Herzegovina. Palaeogeogr. Palaeoclimatol. Palaeoecol. 310, 400–412. http://dx.doi.org/10.1016/j.palaeo.2011.08.001.
de Leeuw, A., Mandic, O., Krijgsman, W., Kuiper, K., Hrvatović, H., 2011b. A chronostratigraphy for the Dinaride Lake System deposits of the Livno-Tomislavgrad Basin: the rise and fall of a long-lived lacustrine environment. Stratigraphy 8, 29–43.
de Leeuw, A., Mandic, O., Krijgsman, W., Kuiper, K., Hrvatović, H., 2012. Paleomagnetic and geochronologic constraints on the geodynamic evolution of the Central Dinarides. Tectonophysics 530–531, 286–298. http://dx.doi.org/10.1016/j.tecto.2012.01.004.
Lorenschat, J., Pérez, L., Correa-Metrio, A., Brenner, M., von Bramann, U., Schwalb, A., 2014. Diversity and spatial distribution of extant freshwater Ostracodes (Crustacea) in Ancient Lake Ohrid (Macedonia/Albania). Diversity 6, 524–550. http://dx.doi.org/10.3390/d6030524.
Mandic, O., Pavelić, D., Harzhauser, M., Zupanič, J., Reischenbacher, D., Sachsenhofer, R.F., Tadej, N., Vranjković, A., 2009. Depositional history of the Miocene Lake Sinj (Dinaride Lake System, Croatia): a long-lived hard-water lake in a pull-apart tectonic setting. J. Paleolimnol. 41, 431–452. http://dx.doi.org/10.1007/s10933-008-9235-1.
Mandic, O., de Leeuw, A., Vuković, B., Krijgsman, W., Harzhauser, M., Kuiper, K.F., 2011. Palaeoenvironmental evolution of Lake Gacko (Southern Bosnia and Herzegovina): impact of the Middle Miocene climatic optimum on the Dinaride Lake System. Palaeogeogr. Palaeoclimatol. Palaeoecol. 299, 475–492. http://dx.doi.org/10.1016/j.palaeo.2010.11.024.
Mandic, O., de Leeuw, A., Bulić, J., Kuiper, K.F., Krijgsman, W., Jurišić-Polšak, Z., 2012. Paleogeographic evolution of the southern Pannonian Basin: $^{40}Ar/^{39}Ar$ age constraints on the Miocene continental series of northern Croatia. Int. J. Earth Sci. 101, 1033–1046. http://dx.doi.org/10.1007/s00531-011-0695-6.
Matenco, L., Radivojević, D., 2012. On the formation and evolution of the Pannonian Basin: constraints derived from the structure of the junction area between the Carpathians and Dinarides. Tectonics 31. http://dx.doi.org/10.1029/2012TC003206.
McFadden, P.L., McElhinny, M.W., 1988. The combined analysis of remagnetization circles and direct observations in palaeomagnetism. Earth Planet. Sci. Lett. 87, 161–172. http://dx.doi.org/10.1016/0012-821X(88)90072-6.
McFadden, P.L., McElhinny, M.W., 1990. Classification of the reversals test in palaeomagnetism. Geophys. J. Int. 103, 725–729. http://dx.doi.org/10.1111/j.1365-246X.1990.tb05683.x.
Mehes, G., 1907. Adatok magyarország pliocen ostracodáinak ismeretéhez. Földtani Közlöny 12, 429–467.
Meisch, C., 2000. Freshwater Ostracoda of Western and Central Europe. Spektrum Akademischer Verlag, Berlin.
Miall, A.D., 1978. Tectonic setting and syndepositional deformation of molasse and other nonmarine-paralic sedimentary basins. Can. J. Earth Sci. 15, 1613–1632. http://dx.doi.org/10.1139/e78-166.
Miall, A.D., 1996. The Geology of Fluvial Deposits. Springer-Verlag, Berlin.
Mikes, T., Christ, D., Petri, R., Dunkl, I., Frei, D., Báldi-Beke, M., Reitner, J., Wemmer, K., Hrvatović, H., Eynatten, H., 2008. Provenance of the Bosnian Flysch. Swiss J. Geosci. 101, 31–54. http://dx.doi.org/10.1007/s00015-008-1291-z.
Milojević, R., 1964. Srednjobosanksog basena - sa naročitim osvrtom na razvoj i ekonomsku vrednost ugljonosnih facija (Middle-Bosnia Coal Basin - With Special Review of Development and Economic Value of Coal-bearing Facies). Belgrade University, Sarajevo.
Milojković, 1929. Stratigrafski pregled geoloških formacija u Bosni i Hercegovini, Izdanje geološkog za Vode u Sarajevu.
Mosbrugger, V., Utescher, T., Dilcher, D.L., 2005. Cenozoic continental climatic evolution of Central Europe. Proc. Natl. Acad. Sci. 102, 14964–14969. http://dx.doi.org/10.1073/pnas.0505267102.
Muftić, M., 1965. Geoloski odnosi ugljonosnih terena Srednjobosanskih ugljenokopa: Bile, Zenice, Kaknja i Breze, Posebna izdanja Geološkog glasnika Sarajevo.
Muftić, M., Luburić, P., 1963. Prilog poznavanju litostratigrafskih i tektonskih odnosa jezerskog neogena u Bosni i Hercegovini. Geološki Glas. Sarajev. 7, 103–130.
Mullender, T.a.T., Velzen, a.J., Dekkers, M.J., 1993. Continuous drift correction and separate identification of ferrimagnetic and paramagnetic contributions in thermomagnetic runs. Geophys. J. Int. 114, 663–672. http://dx.doi.org/10.1111/j.1365-246X.1993.tb06995.x.
Mullender, T.A.T., Frederichs, T., Hilgenfeldt, C., de Groot, L.V., Fabian, K., Dekkers, M.J., 2016. Automated paleomagnetic and rock magnetic data acquisition with an in-line horizontal "2G" system. Geochem. Geophys. Geosyst. 17, 3546–3559. http://dx.doi.org/10.1002/2016GC006436.
Müller, G.W., 1900. Deutschlands Süsswasser-Ostracoden. Zool. Orig. aus dem Gesamgebiete der Zool. 12. pp. 1–112.
Neubauer, T.A., Georgopoulou, E., Kroh, A., Harzhauser, M., Mandic, O., Esu, D., 2015a. Synopsis of European Neogene freshwater gastropod localities: updated stratigraphy and geography. Palaeontol. Electron. 1–7. http://dx.doi.org/10.26879/478.
Neubauer, T.A., Harzhauser, M., Kroh, A., Georgopoulou, E., Mandic, O., 2015b. A gastropod-based biogeographic scheme for the European Neogene freshwater systems. Earth Sci. Rev. 143, 98–116. http://dx.doi.org/10.1016/j.earscirev.2015.01.010.
Neubauer, T.A., Mandic, O., Harzhauser, M., 2015c. The freshwater mollusk fauna of the Middle Miocene Lake Drniš (Dinaride Lake System, Croatia): a taxonomic and systematic revision. Austrian J. Earth Sci. 108, 15–67. http://dx.doi.org/10.17738/ajes.2015.0013.
Olujić, J., Pamić, J., Milojević, R., Veljković, D., Kapeler, I., 1978. Basic Geological Map of the SFRY, 1:000.000, Sheet Vares (L-34-133).
Pálfy, J., Mundil, R., Renne, P.R., Bernor, R.L., Kordos, L., Gasparik, M., 2007. U-Pb and $^{40}Ar/^{39}Ar$ dating of the Miocene fossil track site at Ipolytarnóc (Hungary) and its implications. Earth Planet. Sci. Lett. 258, 160–174. http://dx.doi.org/10.1016/j.epsl.2007.03.029.
Pamić, J., Tomljenović, B., Balen, D., 2002. Geodynamic and petrogenetic evolution of Alpine ophiolites from the central and NW Dinarides: an overview. Lithos 65, 113–142. http://dx.doi.org/10.1016/S0024-4937(02)00162-7.
Pantić, N.K., 1956. Biostratigrafija tercijarne flore Srbije. Geol. An. Balk. Poluostrva 24, 199–321.
Pantić, N., 1961. O starosti slatkovodnog tercijara sa ugljem u Bosni na osnovu paleofloristickih istrazivanja (Über das alter kohlenführenden süsswassertertiärs on Bosnien auf grund von untersuchungen der paläoflora). Ann. Géol. Penins. Balk. XXVIII, 1–19.
Pantić, N.K., 1962. Fosilni ostaci kopnenih biljaka u Jugoslaviji i njihova stratigrafska vrednost, Referati V savjetovanja geologa Jugoslavije. Beograd.
Pantić, N.K., Bešlagić, A., 1964. Palinološke analize mrkog uglja i lignita iz Livanjskog tercijarnog bazena. Geol. An. Balk. Poluostrva 31, 127–133.
Pantić, N., Eremija, M., Petrović, M., 1964. Biostratigrafska analiza miocenske flore i faune iz okoline Ugljevika. Geološki Glas. Sarajev. 10, 27–61.
Pantić, H.K., Erčegovac, M., Pantić, B., 1966. Palinoloska ispitivanja i stratigrafija terestricno-limnockih tercijarnih naslaga u zeničko-sarajevskom basenu. Geol. An. Balk. Poluostrva 32, 183–210.
Pavelić, D., 2001. Tectonostratigraphic model for the North Croatian and North Bosnian sector of the Miocene Pannonian Basin System. Basin Res. 13, 359–376. http://dx.doi.org/10.1046/j.0950-091x.2001.00155.x.

Pavelić, D., Kovačić, M., 1999. Lower Miocene alluvial deposits of the Pozeska Mt. (Pannonian Basin, northern Croatia): cycles, megacycles and tectonic implications. Geol. Croat. 52, 67–76.
Pavelić, D., Kovačić, M., 2018. Sedimentology and stratigraphy of the Neogene rift-type North Croatian Basin (Pannonian Basin System, Croatia): a review. Mar. Pet. Geol. 91, 455–469. http://dx.doi.org/10.1016/j.marpetgeo.2018.01.026.
Pavelić, D., Kovačić, M., Banak, A., Jiménez-Moreno, G., Marković, F., Pikelj, K., Vranjković, A., Premužak, L., Tibljaš, D., Belak, M., 2016. Early Miocene European loess: a new record of aridity in southern Europe. Bull. Geol. Soc. Am. 128, 110–121. http://dx.doi.org/10.1130/B31280.1.
Peryt, T., 1983. Coated Grains. Springer-Verlag, Berlin.
Petrascheck, W., 1952. Der Einfluß der Fazies der Flözablagerung auf die Eigenschaften der Kohle. Zeitschrift der Dtsch. Gesellschaft für Geowissenschaften. 104. pp. 1–9.
Pezelj, Đ., Mandic, O., Ćorić, S., 2013. Paleoenvironmental dynamics in the southern Pannonian Basin during initial Middle Miocene marine flooding. Geol. Carpath. 64. http://dx.doi.org/10.2478/geoca-2013-0006.
Pickford, M., Pourabrishami, Z., 2013. Deciphering Dinotheriensande deinotheriid diversity. Palaeobiodivers. Palaeoenviron. 93, 121–150. http://dx.doi.org/10.1007/s12549-013-0115-y.
Rampnoux, J.P., 1970. Regard sur les Dinarides internes Yougoslaves (Serbie méridionale et Monténégro oriental): stratigraphie, évolution paléogéographie et magmatique. Bull. Soc. Géol. Fr. 7, 948–966.
Riding, R., 1991. Calcareous Algae and Stromatolites. Springer-Verlag, Berlin.
Roberts, A.P., 2015. Magnetic mineral diagenesis. Earth Sci. Rev. 151, 1–47. http://dx.doi.org/10.1016/j.earscirev.2015.09.010.
Rundić, L., 1998. The carapace of fossil ostracodes: paleoenvironmental indicators. Ann. Géol. Penins. Balk. 62, 165–178.
Rundic, L., 2006. Late Miocene ostracodes of Serbia: morphologic and palaeoenvironmental considerations. Geol. An. Balk. Poluostrva (67), 89–100. http://dx.doi.org/10.2298/GABP0667089R.
Sant, K., de Leeuw, A., Chang, L., Czapowski, G., Gąsiew, A., 2015. Paleomagnetic analyses on Badenian-Sarmatian drill cores from the North Carpathian Foredeep (Middle Miocene, Poland). Polish Geol. Inst. Bull. 461, 179–192.
Sant, K., Mandic, O., Rundić, L., Kuiper, K.F., Krijgsman, W., 2018. Age and evolution of the Serbian Lake System: integrated results from Middle Miocene Lake Popovac. Newsl. Stratigr. 51, 117–143. http://dx.doi.org/10.1127/nos/2016/0360.
Šćavničar, S., Krkalo, E., Šćavničar, B., Halle, R., Tibljaš, D., 1983. Naslage s analcimom u Poljanskoj. Zagreb. Rad Jugoslavenske Akad. Znan. Umjet. 404, 137–169.
Schmid, Bernoulli, D., Fügenschuh, B., Matenco, L., Schefer, S., Schuster, R., Tischler, M., Ustaszewski, K., 2008. The Alpine-Carpathian-Dinaridic orogenic system: correlation and evolution of tectonic units. Swiss J. Geosci. 101, 139–183. http://dx.doi.org/10.1007/s00015-008-1247-3.
Sofilj, J., Živanović, M., 1971. Geological Map of the SFRY, 1:100.000, Sheet Prozor (K-33-12).
Sokač, A., 1979. Miocene ostracode fauna at Sinjsko polje. Geol. Vjesn. 31, 137–144.
Sokač, A., Krstić, N., 1987. Ostracode fauna of some non-marine Neogene basins in Yugoslavia. Geol. Vjesn. 40, 45–52.
Stephenson, A., Snowball, I.F., 2001. A large gyromagnetic effect in greigite. Geophys. J. Int. 145, 570–575. http://dx.doi.org/10.1046/j.0956-540x.2001.01434.x.
Stojadinović, U., Matenco, L., Andriessen, P.A.M., Toljić, M., Foeken, J.P.T., 2013. The balance between orogenic building and subsequent extension during the Tertiary evolution of the NE Dinarides: constraints from low-temperature thermochronology. Glob. Planet. Chang. 103, 19–38. http://dx.doi.org/10.1016/j.gloplacha.2012.08.004.
Stow, D.A.V., 2005. Sedimentary Rocks in the Field - a Colour Guide, 5th ed. Manson Publishing.
Tari, V., Pamić, J., 1998. Geodynamic evolution of the northern Dinarides and the southern part of the Pannonian Basin. Tectonophysics 297, 269–281. http://dx.doi.org/10.1016/S0040-1951(98)00172-3.
Tauxe, L., Kent, D.V., 2004. A simplified statistical model for the geomagnetic field and the detection of shallow bias in paleomagnetic inclinations: was the ancient magnetic field dipolar? In: Timescales of the Paleomagnetic. American Geophysical Union, pp. 101–115. http://dx.doi.org/10.1029/145GM08.
Tauxe, L., Watson, G.S., 1994. The fold test: an Eigen analysis approach. Earth Planet. Sci. Lett. 122, 331–341. http://dx.doi.org/10.1016/0012-821X(94)90006-X.
Taylor, M.R., Teichmüller, M., Davis, A., Diessel, C.F.K., Littke, R., Robert, P., 1998. Organic Petrology. Borntraeger, Berlin-Stuttgart.
Toljić, M., Matenco, L., Ducea, M.N., Stojadinović, U., Milivojević, J., Đerić, N., 2013. The evolution of a key segment in the Europe–Adria collision: the Fruška Gora of northern Serbia. Glob. Planet. Chang. 103, 39–62. http://dx.doi.org/10.1016/j.gloplacha.2012.10.009.
Tomljenović, B., Csontos, L., 2001. Neogene-quaternary structures in the border zone between Alps, Dinarides and Pannonian Basin (Hrvatsko zgorje and Karlovac basins, Croatia). Int. J. Earth Sci. 90, 560–578. http://dx.doi.org/10.1007/s005310000176.
van Unen, M., Matenco, L., Nader, F., Darnault, R., Mandic, O., Tomljenovic, B., Demir, V., 2017. Lateral transfer of Neogene contractional deformation in the Dinarides during the Adriatic indentation. In: Geophyscial Research Abstracts - EGU2017, pp. 1.
Ustaszewski, K., Schmid, S.M., Fügenschuh, B., Tischler, M., Kissling, E., Spakman, W., 2008. A map-view restoration of the Alpine-Carpathian-Dinaridic system for the Early Miocene. Swiss J. Geosci. 101, 273–294. http://dx.doi.org/10.1007/s00015-008-1288-7.
Ustaszewski, K., Kounov, A., Schmid, S.M., Schaltegger, U., Krenn, E., Frank, W., Fügenschuh, B., 2010. Evolution of the Adria-Europe plate boundary in the northern Dinarides: from continent-continent collision to back-arc extension. Tectonics 29, TC6017. http://dx.doi.org/10.1029/2010TC002668.
Ustaszewski, K., Herak, M., Tomljenović, B., Herak, D., Matej, S., 2014. Neotectonics of the Dinarides-Pannonian Basin transition and possible earthquake sources in the Banja Luka epicentral area. J. Geodyn. 82, 52–68. http://dx.doi.org/10.1016/j.jog.2014.04.006.
Utescher, T., Djordjevic-Milutinovic, D., Bruch, A., Mosbrugger, V., 2007. Palaeoclimate and vegetation change in Serbia during the last 30 Ma. Palaeogeogr. Palaeoclimatol. Palaeoecol. 253, 157–168. http://dx.doi.org/10.1016/j.palaeo.2007.03.037.
Vasiliev, I., Franke, C., Meeldijk, J.D., Dekkers, M.J., Langereis, C.O.R.G., Krijgsman, W., 2008. Putative greigite magnetofossils from the Pliocene epoch. Nat. Geosci. http://dx.doi.org/10.1038/ngeo335.
Welter-Schultes, F.W., 2012. European Non-marine Molluscs, a Guide for Species Identification. Planet Poster Editions, Göttingen.
Wessels, W., Markovic, Z., de Bruijn, H., Daxner-Hock, G., Mandic, O., Sisic, E., 2008. Paleogeography of Late Oligocene to Miocene rodent assemblages from the western Dinaride-Anatolian. In: EGU General Assembly, Geophysical Research Abstracts, pp. 1–2.
Weyland, H., Pflug, H., Pantić, N., 1958. Untersuchungen über die Sporen und Pollen-Flora einige jugoslawischer und griechischer Braunkohlen. Palaeontographica 105, 75–99.
Whelan, J., Farrington, J.W., 1992. Organic Matter - Productivity, Accumulation, and Preservation in Recent and Ancient Sediments. Columbia University Press, New York.
Witt, W., 2002. Zur Süßwasserostracodenfauna der oligo-miozänen Vorlandmolasse Süddeutschlands. Min. Bayer. Staatsslg. Paläont. Hist. Geol. 42, 35–39.
Witt, W., 2011. Mixed ostracod faunas, co-occurrence of marine Oligocene and non-marine Miocene taxa at Pınarhisar, Thrace, Turkey. Zitteliana 51, 237–254.
Zachos, J., Pagani, M., Sloan, L., Thomas, E., Billups, K., 2001. Trends, rhythms, and aberrations in global climate 65 Ma to present. Science 292, 686–693. http://dx.doi.org/10.1126/science.1059412.
Zijderveld, J.D.A., 1967. Demagnetization of rocks: analysis of results. In: Collinson, D.W., Creer, K.M., Runcom, S.K. (Eds.), Methods in Paleomagnetism. Elsevier, Amsterdam, pp. 254–286.
Živanović, M., Sofilj, J., Milojević, R., 1967. Basic Geological Map of the SFRY, 1:100.000, Sheet Zenica (L-33-144).
Županić, J., Babić, L., 2011. Sedimentary evolution of an inner foreland basin margin: Paleogene Promina Beds of the type area, Mt. Promina (Dinarides, Croatia). Geol. Croat. 64, 101–120. http://dx.doi.org/10.4154/gc.2011.09.